Non-cylindrical parasitic folding and strain partitioning during the Pan-African Lufilian orogeny in the Chambishi-Nkana Basin, Central African Copperbelt

Koen Torremans[1], Philippe Muchez[1], Manuel Sintubin[2]

[1]KU Leuven, Department of Earth and Environmental Sciences, Geodynamics and Geofluids Research Group, Celestijnenlaan 200E, 3001 Leuven, Belgium.
[2]Present address: Irish Centre for Research in Applied Geosciences, University College Dublin, Dublin 4, Ireland.

Correspondence to: Koen Torremans (koen.torremans@icrag-centre.org)

Abstract. A structural analysis has been carried out along the southeast margin of the Chambishi-Nkana Basin in the Central African Copperbelt, hosting the world-class Cu-Co Nkana orebody. The geometrically complex structural architecture is interpreted to have been generated during a single NE-SW oriented compressional event, clearly linked to the Pan-African Lufilian orogeny. This progressive deformation resulted primarily in asymmetric multiscale parasitic fold assemblages, characterized by non-cylindrical NW-SE oriented periclinal folds that strongly interfere laterally, leading to fold linkage and bifurcation. The vergence and amplitude of these folds consistently reflect their position along an inclined limb of a NW plunging megascale first-order fold. A clear relation is observed between the intensity of parasitic folding and the degree of shale content in the Copperbelt Orebody Member, which hosts most of the ore. Differences in fold amplitude, wavelength and shape are explained by changes in mechanical stratigraphy caused by lateral lithofacies variation in ore-bearing horizons. In addition, strong differences in strain partitioning occur within the deforming basin, which is interpreted to be in part controlled by changes in mechanical anisotropy in the layered rock package. This work provides an essential backdrop to understand the influence of the Lufilian orogeny on metal mineralization and (re−)mobilization in the Copperbelt.

1 Introduction

The Central African Copperbelt is the largest and highest-grade sediment-hosted copper and cobalt (Cu−Co) producing metallogenic province in the world (Fig. 1). It hosts over 80 deposits with more than 152 million metric tonnes of contained Cu (Zientek et al., 2010) or c. 200 million metric tonnes according to Hitzman et al., (2012), as well as the largest Co reserves in the world (>60%). Metallogenesis in the Central African Copperbelt is generally seen as a multi-stage and often deposit-specific process with at least some of the following: Diagenetic mineralization pulses are followed by multiple remobilization stages (including potential new mineralization) related to basin inversion and compressional deformation, as well as later supergene enrichment (e.g. Cailteux et al., 2005; Selley et al., 2005; Dewaele et al., 2006; Haest and Muchez 2011; Hitzman et al., 2012).

Many unknowns remain on the exact nature of compressional deformation in many areas of the Copperbelt, despite the obvious importance with regard to deformation and mobilization of ore and potential for new input of metals. In the Eastern Middle Lufilian ('Zambian Copperbelt'; Figs. 1 and 2), some of the ore within the deposits is strongly structurally controlled (Brock 1961; Daly et al., 1984; Selley et al., 2005; Hitzman et al., 2012; Eglinger et al., 2013; Turlin et al., 2016). Ore is for example localized along thrust fault-propagation folds or detachment structures at Nchanga (for location see Fig. 2; McGowan et al., 2003, 2006). At Nkana, ore appears enriched in fold hinges, along tectonic cleavage planes or in several generations of fold-

related veins, in addition to disseminated and lenticular ore (for location see Fig. 2; Brems et al., 2009; Croaker 2011; Torremans et al., 2014).

The focus of this study is the Nkana Cu-Co deposit, one of the world-class Cu-Co orebodies in the Eastern Middle Lufilian (Fig. 2). Unequivocal evidence for early diagenetic Cu-Co mineralization is lacking, which does not exclude its existence (Brems et al., 2009; Muchez et al., 2010). At Nkana South, several mineralization/remobilization stages have been identified from basin inversion onwards, characterized by different vein generations that formed during compressional deformation (Muchez et al., 2010; Torremans et al., 2014). Geological mapping has indicated that rich orebodies are present in the hinge zones of tight to isoclinal folds, both at Nkana South (Brems et al., 2009) and Nkana Central (De Cleyn 2009). Conversely, at Mindola, the ore occurs in beds that are simply dipping to the SW without significant folding (for location see Fig. 2; Clara 2009). A significant lateral variation is hence observed in the way mineralization occurs in relation to geological structures along the Chambishi-Nkana Basin (Fig 2; Muchez et al., 2010).

Despite many insights into the metallogenetic processes, a detailed structural framework for the Nkana deposit is still missing. Such a framework is nevertheless paramount in order to assess the relation between compressional deformation and mobilization of the ores and potential input of new ore, and to explain the lateral variation in the occurrence of the ore at Nkana and similar deposits in one of the great metallogenic provinces of the world. The purpose of this paper is therefore to provide a regional and deposit-scale structural and stratigraphic framework, and to provide general insights into fold-related deformation and the influence of mechanical stratigraphy, in particular with respect to non-cylindrical and parasitic folding and strain partitioning.

2 Geological and Geodynamic Setting

2.1 Regional geodynamic context

The geodynamic evolution of the Central African Copperbelt can be roughly subdivided into continental rifting leading to development of the extensional basin, subsequent proto-oceanic rifting and ultimately inversion and compressional tectonics followed by post-orogenic cooling.

The rocks in the study area belong to the Neoproterozoic to early Cambrian Katanga Supergroup (Fig. 1, 2). Basement rocks to the Katanga Supergroup are exposed in the Kafue basement inlier and smaller surrounding inliers, consisting of the Lufubu and Muva Supergroups (Garlick 1961a; Mendelsohn 1961; Daly and Unrug 1982; Johnson et al., 2005; De Waele et al., 2006). The Muva Supergroup quartzites and extensive pre-Katanga granitoids represent positive elements in the current and palaeotopography (Mendelsohn 1961). The Katanga Supergroup nonconformably overlies these basement rocks. The basement rocks are intruded by various pre-Katangan granites. The youngest intrusive body into basement rocks is the A-type

Nchanga Red Granite, of which magmatic zircons in quartzite of the Katanga Supergroup were dated at 883 ± 10 Ma by U–Pb SHRIMP (Armstrong et al., 2005). This age provides a maximum age for sedimentation of the Katanga Supergroup which is further subdivided in the Roan, Nguba and Kundelungu Groups (Cailteux et al., 1994).

The lowermost Mindola Clastics Formation of the Roan Group contains conglomerates, sandstones and arkoses that were deposited during intracratonic continental rifting in fault-bounded sub-basins (Tembo et al., 1999; Bull et al., 2011). Subsequently, the overlying Copperbelt Orebody Member (COM) – often referred to as the Ore Shale and part of the Kitwe Formation, represents the first transgressive surface above the red-bed sediments of the Mindola Clastics Formation. The rest of the Kitwe Formation marks rift climax with concomitant fault linkage interpreted as a sag-phase in the rifting (Cailteux et al., 1994; Selley et al., 2005; Batumike et al., 2007; Bull et al., 2011). The evaporate-rich upper Roan Group and Mwashya Group reflect more quiescent conditions in basin development (Cailteux et al., 1994, 2007; Porada and Berhorst 2000; Selley et al., 2005; Bull et al., 2011).

The overlying Nguba and Kundulungu Groups contain carbonate and siliciclastic rocks with two regionally extensive basal glaciogenic diamictites (Batumike et al., 2006, 2007). These units reflect continued basin development that lead to proto-oceanic rifting of Afar/Red Sea type (Kampunzu et al., 1991, 2000; Tembo et al., 1999; Porada and Berhorst 2000; Key et al., 2001; Batumike et al., 2007). Widespread small gabbroic to dioritic sills and dykes occur in the Katangan Supergroup (Fig. 2, 3), in particular in the Upper Roan and lowermost Nguba Groups (Kampunzu et al., 2000). These mafic bodies are constrained between c. 735 and 765 Ma (Key et al., 2001; Barron et al., 2003), also presenting an approximate age for the extensional tectonics associated with this rifting phase (Buffard 1988; Tembo et al., 1999; Kampunzu et al., 2000; Batumike et al., 2007).

Inversion from extensional to compressional tectonics during the Pan-African orogeny led to formation of the northward convex Lufilian oroclinal belt (Cosi et al., 1992; Kampunzu and Cailteux 1999; Porada and Berhorst 2000). Its arcuate shape (Fig. 1) has recently been interpreted as being the result of orogenic bending only after development of the first compressional brittle structures in the orogen (Kipata et al., 2013), although the origin of the bending still remains a matter of discussion (Daly et al., 1984; Kampunzu and Cailteux 1999; Porada and Berhorst 2000; Jackson et al., 2003; Selley et al., 2005). Variable deformation styles are observed throughout the arc, both transverse and parallel to the structural grain (Cosi et al., 1992; Jackson et al., 2003; Eglinger et al., 2016; Turlin et al., 2016). Therefore, the Lufilian Arc is often subdivided in different tectonic domains (Fig. 1). Of interest here are the Outer Lufilian ('external fold-and-thrust belt'), the Western Middle Lufilian ('Domes region') and the Eastern Middle Lufilian ('Zambian Copperbelt') (De Swardt and Drysdall 1964; Daly et al., 1984; Jackson et al., 2003; Selley et al., 2005). In the Eastern Middle Lufilian zone, both around and farther north of the Kafue basement inlier, deformation in the Katanga Supergroup is mainly by folding (Porada and Berhorst 2000; Selley et al., 2005). Only in some localities have shear zones involving both Katanga Supergroup and basement rocks been observed (Coward and Daly 1984; Daly et al., 1984; McGowan et al., 2006).

The precise timing of tectono-metamorphic events related to basin evolution and the Lufilian orogeny is still under-constrained, in particular in the Eastern Middle Lufilian (Fig. 3). Inversion and deformation of the Katanga basin occurred during the Lufilian Orogeny starting from 560 to 500 Ma (Hitzman et al., 2012), with the main phase of the orogeny estimated between 560 to 530 Ma (Selley et al., 2005). The Katanga Supergroup in the study area was metamorphosed to greenschist and lower amphibolite facies, with biotite/phlogopite and tremolite as main metamorphic minerals (Brems et al., 2009). The metamorphic grade and the general lack of datable minerals makes it difficult to directly date tectono-metamorphic events affecting the basinal rocks. A peak-metamorphic 531 ± 12 Ma U–Pb monazite age was obtained by Rainaud et al. (2005a) for the Chambishi-Nkana Basin in the Eastern Middle Lufilian. Talc-kyanite whiteschists along the contact between basement and Katangan Supergroup rocks record peak metamorphism in the Western Middle Lufilian in NW Zambia (Cosi et al., 1992; Broughton et al., 2002; Eglinger et al., 2016). These high pressure whiteschists are constrained by a 529 ± 2 Ma monazite age and 524 ± 3 Ma to 532 ± 2 Ma U–Pb ages (John et al., 2004; Eglinger et al., 2016) and indicate crustal burial, exhumation and thrust stacking of migatitic basement and Katangan rocks, linked to closure of a southern ocean basin during the Lufilian oreogeny (Coward & Daly, 1984; Cosi et al., 1992; Porada & Berhorst, 2000; John et al., 2004). Peak metamorphic ages are therefore quite consistently around 530 to 525 Ma along the entire Middle Lufilian (Fig. 3). Authigenic muscovite and biotite ^{40}Ar–^{39}Ar and Rb/Sr ages of c. 498 to 465 Ma are interpreted to represent post-orogenic cooling (John et al., 2004; Rainaud et al., 2005a) in agreement with the 510 to 450 Ma Rb/Sr muscovite ages from Cosi et al., (1992).

2.2 The Chambishi-Nkana Basin and Nkana Cu-Co deposit

The Nkana Cu-Co deposit is situated near Kitwe in the Eastern Middle Lufilian (Zambian Copperbelt; Figs. 1, 2). It lies to the west of the Kafue basement inlier, often referred to as the Kafue Anticline (Selley et al., 2005; Hitzman et al., 2012). More specifically, the mine lies on the southeastern margin of the Chambishi-Nkana Basin which is a synclinorium consisting of a succession of 10^3-10^4 m amplitude folds, around 40 km at its widest (Figs. 2, 4). Here, Katanga Supergroup metasediments are surrounded by a variable suite of basement rocks (Bard and Jordaan 1963). A large scale SW verging syncline with a wavelength of c. 6 km is developed on the southeast termination of the Chambishi-Nkana Basin (Fig.4; Bard and Jordaan 1963; Brems et al., 2009). The study area is situated on the eastern limb of this syncline which closes to the SE in the Nkana South area.

Nkana is a stratiform deposit in the sense that most of the ore is found near the base of the 10 to 20m thick COM. Minor ore also occurs at the top of the underlying Mindola Clastics Fm and at the base of hangingwall units overlying it. Mineralization occurs as disseminated sulfides in the host rock, in several generations of veins and associated with structures such as hinge zone of tight to isoclinal folds, deformed veins, faults, and burial or tectonic foliations (Brems et al., 2009; Torremans et al., 2014). Several mineralization/remobilization stages have been identified at Nkana (Brems et al., 2009; Muchez et al., 2010).

Because of the strong deformation and remobilization stages, diagenetic mineralisation is often destroyed or replaced, but is generally assumed to be a significant precursor to the current orebody (Brems et al., 2009; Muchez et al., 2010). Current metallogenetic models as well as Pb, Sr and Nd isotope data indicate that felsic and mafic basement rocks in the Domes region and the overlying sediments constitute the most likely source area for metals (Carr et al., 1987; Selley et al., 2005; Van Wilderode et al., 2015). The deposit is developed from 4 shafts: Mindola North, Mindola, Nkana Central and Nkana South. Mining operations at Nkana Central and South are contiguous for 6.1 km along strike. To the north, Mindola and Mindola North comprise an additional 6.4 km, separated from Nkana Central by the 1.2 km Kitwe barren gap and bounded to the north by the Ichimpe barren gap (Fig. 4).

3 Methodology

Multiple outcrops were studied 14 km along strike the southeastern margin of the Chambishi-Nkana syncline (number 1 to 14 in Fig. 4). A list of structural measurements, boreholes and sections that were used in this study is given with position data in the online supplementary material. The focus was put on deformation features in the COM and closely adjacent parts of under- and overlying formations. OpenStereo was used to process some of the structural data (Grohmann and Campanha 2010). To test for preferred orientations or randomness in the 3D data, the eigenvalue technique of Woodcock and Naylor (1983) was used. Here, parameters K and C are strength and shape parameters respectively. Low and high K values indicate girdle distributions or clustered data, respectively. The strength parameter C indicates the strength of the preferred orientation in the data sample. Values of K = 1 and C = 0 are completely randomly distributed. Petrography was performed on polished thin sections, thick doubly polished wafers and polished sections. Petrographic and microstructural observations were carried out on 82 oriented thin sections that were obtained in a 2012 field campaign, in addition to 76 thin sections and and 35 polished sections available from an extensive sample collection of two previous studies at Nkana (Brems et al., 2009; Muchez et al., 2010).

4 Lithofacies Variation in the Copperbelt Orebody Member at Nkana (COM)

The COM is characterized by strong lateral lithofacies variations, resulting in a variable carbonate versus siliciclastic content and grain size (Annels 1989; Cailteux et al., 1994; Selley et al., 2005; Bull et al., 2011). The term lithofacies is used as a distinct set of mappable units on the mine scale, based on a petrographical study. Four main lithofacies assemblages are recognized in the COM at the Nkana deposit, representing sections through the COM at different localities in the Nkana deposit (Fig. 5). The first-order spatial distribution of the different lithofacies is indicated in Figure 4. From north to south (Fig. 4) the COM is characterized subsequently by (1) strongly cemented argillaceous dolomites at Mindola, (2) massive dolomites in the

Kitwe Barren Gap, (3) turning into a transitional lithofacies north of Nkana Central (also noted by Bard and Jordaan 1963) and (4) ultimately gradually changing to a carbonaceous mudrock lithofacies with high fissility at Nkana Central and South. Several patches of transitional lithofacies are present in various areas of Nkana South and Central.

4.1 Carbonaceous mudrock lithofacies

This lithofacies assemblage consists of carbonaceous dark grey to black laminated to finely bedded pelites and siltstones. A pronounced shaly fabric is often developed, explaining why the mudrocks have been termed "Ore Shale" member or formation in the majority of the literature. Petrographic study shows that the mineralogy consists of quartz, muscovite, biotite, dolomite, K-feldspar (mainly microcline), and minor orthoclase, pyrite and chalcopyrite, bornite and pyrrhotite and accessory apatite and zircon (also cf. Brems et al., 2009; Muchez et al., 2010). Abundant organic matter occurs in the host rock, in the form of disseminated solid bitumen inclusions elongated along shaly cleavage. Total organic carbon contents in whole-rock analyses at Nkana South are between 0.13% and 3.54% (Selley et al., 2005; Croaker 2011). Accessory layers with fine-grained sandstone are found, mainly containing quartz.

4.2 Argillaceous dolomite lithofacies

The argillaceous dolomite lithofacies can be subdivided into seven units that are used in the mine as marker horizons (Fig. 5). This lithofacies assemblage consists of laminated to thinly bedded argillaceous dolomite with a variable dolomite content. Dolomite content peaks in units 3 and 5 and gradually diminishes stratigraphically upwards. Where dolomite content is low (units 2 and 6), lithologies are pure clay- and siltstones, either laminated to interbedded or massive and homogeneous. Dolomite-quartz nodules with pyrite and chalcopyrite occur and are particularly persistent in units 6 and 7, and of minor importance in units 1 and 2. Chickenwire textures reminiscent of pseudomorphosed gypsum or anhydrite, load casts and dewatering structures occur throughout, most often in units 1, 2 and 4. Bedding in units 1, 3 and 5 is often wavy and contorted (Fig. 6E, F). The top unit (COM7 on Fig. 5) and transition towards meta-arkoses and quartzites of the Rokana Evaporites Member are similar across the entire deposit, regardless of lithofacies assemblage.

4.3 Transitional lithofacies

Laterally, the carbonaceous mudrock lithofacies transitions into a dolomitized siltstone to fine-grained sandstone lithofacies. Generally, this transition is situated one km north of Nkana Central (Fig. 4), however, patches of transitional lithofacies are found in places around Nkana Central (e.g. borehole CE555 in Nkana Central at 100mN). The argillaceous dolomite and carbonaceous mudrock are therefore end-member cases of a lithological continuum.

4.4 Massive dolomite lithofacies

Other lithofacies associations are recognized at Nkana. The most important is a massive white, occasionally siliceous dolomite, intensely studied by other authors (Bard and Jordaan 1963; Clemmey 1974, 1978; Annels 1989; Croaker 2011). These studies and other (Selley et al., 2005; Bull et al., 2011) have found that massive dolomite bodies are associated with so-called subeconomic barren gaps in the COM and always lies on inferred basement palaeohighs. Examples of this are the Kitwe barren gap between Nkana Mindola and Nkana Central and the Ichimpe barren gap to the north of Nkana Mindola (Fig. 4). In these places, the Mindola Clastics Formation is much thinner to almost non-existent and transitions towards the lithofacies association at Nkana Mindola are very rapid (Jordaan 1961; Selley et al., 2005). Important alteration by talc, tremolite and anhydrite sometimes affects this dolomite (Porada and Berhorst 2000; Croaker 2011; Bull et al., 2011).

4.5 Gradual change stratigraphically upward towards lithologies that are uniform across the study area

At all localities a gradual transition is seen towards a more interbedded dark grey calcitic siltstone to fine-grained calcarenite towards the top of the COM (Fig. 5). In addition, at the top, nodules up to 10 cm in diameter occur in the matrix that reveal strain shadows of dolomite and quartz elongated parallel to local tectonic cleavage. The top of the Mindola Clastics Formation directly beneath the COM occasionally shows dolomitized crossbedding. The lowermost part of the COM generally consists of a strongly altered sequence of variable thickness, named the "Contact Shale".

5. Structural analysis

5.1 Foliations and structural polarity

A strong, bedding-parallel, shaly cleavage, S_1, is developed in the carbonaceous mudrock to siltstone lithofacies of the COM (Fig. 6I). In the argillaceous dolomite at Nkana Mindola, S_1 is generally not strongly developed (Fig. 6F). Gradual appearance of this shaly cleavage coincides with the lithofacies transition towards carbonaceous mudrock southwards of Nkana Central. Generally, the tectonic S_2 cleavage is not as strongly developed as S_1 in the incompetent layers of the carbonaceous mudrock lithofacies of the COM (Fig. 6I). Here, S_2 cleavage is developed by the diffuse and discontinuous alignment of micas and sulfides, with occasional S_2-parallel authigenic dolomite and quartz grains. In the argillaceous dolomite, S_2 is mainly visible by strong alignment of disseminated micas and sulfides in siliciclastic layers and especially prominent in layers of replacive coarse-grained dolomite.

Locally, a strong disjunctive and anastomosing S_2 cleavage is developed in the highest strain domains of the carbonaceous mudrock lithofacies at Nkana Central and South (throughout southern parts of the study area, in outcrops 6, 7, 10 and 12 at Nkana South, but also in outcrop 5 at Nkana Central; Fig. 4). Cleavage spacing is in the order of several centimeters up to 10

or 20 cm and abundant Cu−Co sulfides or micas are aligned along these cleavage planes. The S_2 cleavage is particularly pronounced when it parallels S_1, i.e. at 230/90. Often, transposition occurs of ptygmatically folded S_1-cleavage-parallel veins, showing pinch-and-swell or boudinage parallel to the S_2 cleavage. Bedding-cleavage S_1-S_2 angular relationships and stratigraphic way-up structures, such as trough crossbedding and scours in the top of the Mindola Clastics Formation show concordant structural and stratigraphic polarity. Antiforms are thus anticlines, synforms synclines. The quartzites and arkoses of the overlying Rokana Evaporates Member and underlying Mindola Clastics Formation do not show significant macroscopic cleavage. The S_1-S_2 intersection lineation (Li) could only be confidently measured in the Nkana South open pit and was difficult to measure in underground crosscuts through the COM.

5.2 Folds

5.2.1 Multiple order folds along the eastern limb of the Chambishi-Nkana syncline

The Chambishi-Nkana syncline is shallowly plunging to the northwest, showing an undulatory profile with successive axial depressions and culminations (Fig. 4; Jordaan 1961). It reverses its plunge when approaching the north-western side of the Chambishi-Nkana Basin at the Chambishi and Mwambashi B mines (Fig. 2; Bard and Jordaan 1963; Selley et al., 2005; Brems et al., 2009). Many <100m scale 2nd order folds are developed along this 1st order fold. The outcrop patterns of these 2nd order folds show M-type folds in the southeast and S- or Z-type folds on the southwest and northeast limbs of the 1st order syncline, respectively (Fig. 4). In turn, the 2nd order folds are decorated by 3rd order folds on the scale of several meters, mainly developed in the more competent Rokana Evaporites Member and Nchanga Quartzite Member (Fig. 6A, B). Ultimately, 4th order folds reveal wavelengths of centimeter to decimeter scale, predominantly developed in the COM (Figs. 7A-D).

In the carbonaceous mudrock lithofacies, pre-folding bedding-parallel fibrous dolomite veins and subsequent overgrowth generations are often strongly buckled and folded or sheared into 4th order folds (Fig. 6D; Torremans et al., 2014). Certainly in the hinges of 2nd and 3rd order folds, these parasitically folded closely spaced veins show high amplitude M-type folds (Fig. 6D). Conversely, veins of similar spacing in the limbs of 2nd and 3rd order folds generally show a smaller amplitude, a strong vergence towards the fold hinge of the lower order folds and parallelism of fold axial planes with the lower order folds (Fig 7A, B).

Many bedding surfaces in the COM and Rokana Evaporites Member show slickensides with mica, chlorite and tremolite fibres and abundant bedding-parallel slickenfibre veins. These slickenlines have a pitch between 70° and 90° and are orthogonal to local fold hinge lines and π-axis-to-S_1-cleavage (Fig. 6G, H). Lineations formed by the slickenfibre step edges are close to sub-horizontal (max plunge 20° NW or SE) and therefore parallel to the local π-axis-to-S_1-cleavage (Fig. 6G, H). At Mindola, dolomite slickenfibre-veins are predominantly present in dolomite-rich coarser-grained units 1, 3 and 5.

Folds at Nkana South (sections 6−12): Deca- to hectometer scale 2nd order folds characterize sections 6 to 12 at Nkana South (Fig. 4). These folds are upright to occasionally overturned with slight NE verging asymmetry and tight to isoclinal interlimb angles. Fold trains show wavelengths of c. 50 m and a succession of such folds is seen in the Nkana South open pit (section 8 in Figs. 8 and 9) and underground for sections 7 to 9 (Fig. 10D-F). Third order M-, S- and Z-type folds are developed on the northeast verging 2nd order folds in the Rokana Evaporites Member and the Kafue Arenites Member (section 8; Fig. 6A-C). Occasionally, pinch-and-swell geometries are observed in overturned limbs. At Nkana South and Central abundant bedding-parallel veins show single-layer or dis- and polyharmonic multilayer 4th order folds with wavelengths between 0 and 40 cm (Fig. 6D).

Foliations in the COM are strongly clustered, which is reflecting that the COM is often isoclinally folded with high aspect ratios between fold amplitude and wavelength (>3) (zones 3 and 4 in Fig. 8B, 9). For example, measured S2 values for section 8 are strongly (C = 4.12) clustered (K = 2.98) with a mean plane at 219/84 (Fig. 8). In addition, poles-to-S_1-cleavage are also strongly clustered around 19/038 (Fig. 8). Intense fold hinge thickening is seen in the COM (Fig. 9) leading to class 1C folds (Ramsay 1967).

Conversely, in the formations overlying the COM poles-to-S1-cleavage of individual folds show great-circle β-girdle distributions (dashed lines for section 8 in Fig. 8). For the entire fold sequence at the Nkana South open pit, the mean β-girdle of all combined poles-to-S_1-cleavage yields an attitude of 87/138 with a girdle-like distribution, as indicated by a shape parameter K of 1.29 with a strength C of 2.96 (Woodcock and Naylor 1983). The pole of this β-girdle plunges 03/318 (Fig. 8). The S_2 cleavage is always axial planar to the folds. Marginal fanning and refraction of S_2 cleavage is occasionally seen across folds in metapelites in COM unit 7, or in overlying formations although the refraction angle is very small (Fig. 6C). Poles-to-S_2-cleavage show slight NE vergence of axial planes, as indicated by the mean S_2 cleavage plane (84/219) and its pole to mean S_2 cleavage (06/039). The intersection lineation is quite variably sub-horizontal to gently NW or SE plunging. On average, Li plunges 299/08 in section 8 (Figs. 4, 8).

Folds at Nkana Central and Mindola (sections 1−5): 2nd order folds gradually become more open to the north of Nkana Central shaft and show progressively lower wavelengths and interlimb angles northwards. The lateral spacing between 2nd order anticlinal fold hinges decreases from less than 100 m near Nkana South (Figs. 9, 10B) to several hundreds of meters near Nkana Central (Figs. 10C, 11) For example, the 2nd order folds in outcrops 4 and 5 are developed on a scale of several hectometer. Similarly, the anticline in outcrop 13 shows a moderately open fold developed on the scale of 500-600 m (Fig 11B). Parasitic fold development on the limbs of 2nd order folds is also less frequent and at lower amplitudes and wavelengths than at Nkana South. Although folds are more open at Nkana Central, angular fold hinges also characterize the COM (Fig. 11B). The strike of the folds is somewhat more north-directed, as indicated by the π-axis-to-S_1-cleavage and the S_2 cleavage

(section 5 in Fig. 4). Folds in section 5 are shallowly plunging with the π-axis-to-S_1-cleavage plunging 04/348 and with a fold hinge line plunging 07/345 (Fig. 4).

At the northernmost side of Mindola, beds are broadly warping on the northern normal limb of the 1st order syncline, as shown by poles-to-bedding in Figure 4. Here, many asymmetrical 4th order intraformational folds are observed, particularly in units 1, 3 and 5 of the COM (Fig. 6E, F). These folds are mainly developed by the thin silty layers (up to 3 cm thick) with intermittent dolomite showing considerable thickness variations in between folded siltstone bands. The fold trains show dis− to polyharmonic multilayer folding but also change laterally from straight undeformed segments into folded segments (Fig. 6E, F). Many of the siltstone and dolomite bands are also broken up (Fig. 6F). These intraformational folds consistently reveal subvertical to slightly N-verging axial planes clearly expressed by an S_2 cleavage, along which sulfides are aligned (Fig 6F).

5.2.2 Non-cylindrical periclinal fold geometries

At Nkana South and Central, 2nd and 3rd order folds are non-cylindrical and often doubly plunging. A doubly plunging fold hinge line was directly observed in section view on the SW face of the Nkana South open pit (section 8). Here, the intersection lineation varies between gently NW or SE plunging, averaging 299/08, and the total variation in Li and π-axes-to-S_1-cleavage is c. 15° (Fig. 8), which is a similar spread as for the entire Chambishi-Nkana Basin (Fig. 12). Importantly, the abundant 3rd and 4th order folds plunge in the same direction as their parent 2nd order anticline (Fig. 8). Similarly, the π-axes-to-S_1-cleavage plunge both to the NW and SE for several outcrops along the eastern margin of the Chambishi-Nkana Basin (Fig. 4). Doubly plunging folds and undulating fold hinge lines lead to elongate periclinal dome-shaped geometries in geological maps near outcrops 7 and 9 (Fig. 10).

The periclinal fold geometries at Nkana interact along strike, leading to fold linking and bifurcation. The different possible types of fold linkage are exemplified in Fig. 10A-C. A first example of fold bifurcation occurs at outcrop 13 near Nkana Central (Fig. 6B). Initially, at 1500N, a moderately open 2nd order fold is developed on the scale of 500-600 meter, with a fold hinge line plunging 07/345. A small 3rd order anticline-syncline pair is developed on the SW limb of this 2nd order anticline (Fig. 11B). Down plunge, this parasitic fold gains amplitude and wavelength to become a 2nd order fold plunging c. 10° in the same direction. Concomitantly, the northern anticline decreases in size. Ultimately, at 3000N, the two anticlines are equal in amplitude and wavelength. This structure can therefore be seen as a left lateral bifurcated anticline by lateral linkage of one fold with two other folds (Ghosh and Ramberg 1968). A second example, at outcrop 14, reveals complex fold patterns in a fold train of parasitic 3rd order folds along the southwestern limb of a 2nd order fold (Fig. 11A). This parasitic fold train gradually decreases in importance towards the northwest, dying out on the limbs of the lower order fold. As a final example, the geological map of 3360L mining level at Nkana South published by Brems et al., (2009) shows curved axial traces, elongate periclinal folds and both lateral en-echelon linkage and bifurcation fold linkage (vertically below outcrop 8; Fig. 10C). Previous

studies at Nkana have identified similar variability in fold hinge lines with plunges between 20° to 40° northwest and local steepening, flattening and reversing of fold hinge attitudes (Jordaan 1961; Bard and Jordaan 1963). Many of the periclinal fold geometries are hence arranged as a left or right lateral en-echelon series of folds, showing bifurcation linkage or en-echelon linkage, with frequent asymmetric structural saddles in between 2nd order folds.

5.3 Faults and shear zones

Low angle reverse faults are recognized in the Mindola Clastics and Kitwe Formations at Nkana South and Central. Two well-exposed low-angle reverse faults at outcrop 9 reveal 10 m fault displacements at an angle of 15°, yielding stratigraphic displacements of up to 3 or 4 m (Fig. 7D). These low-angle faults show laminated veins parallel to the fault surface and cut off folded bedding-parallel veins and disjunctive S_2 cleavage planes (Fig. 7D). Fault movements are almost pure dip-slip, with a pitch of 85S for talc slickenlines on a 215/33 fault and 87S for tremolite slickenlines on a 203/13 fault.

In addition to these low-angle reverse faults, high angle faults are observed, mostly with normal and rarely with a reverse shear sense. Fig. 7E shows such a steeply dipping fault at outcrop 7, with inferred normal shear sense from several subvertical arrowhead veins with high aspect ratios that straddle the fault surface. The fault is also marked by fault-parallel laminated veins. Similar examples are found in outcrops 8 and 10. Displacements along individual faults are small, on the decimeter to cm scale, also for higher levels at the Nkana deposit (Jordaan 1961; Bard and Jordaan 1963).

At Nkana South and Central, S_2 cleavage planes in the high-strain areas reveal evidence of shear. In the hinge zones of high strain chevron folds, steeply inclined shear zones in the COM are found sub-parallel to axial planar S_2 cleavage.

5.4. Mineralization in relation to structural elements

In the carbonaceous shale, sulfides are generally aligned with S_2 cleavage, be it as disseminated sulfides elongated parallel to S_2 or as stringers and layers along more pronounced S_2 cleavage planes (Fig. 7B). The same is true for sulfides in the host rock of the argillaceous dolomite lithofacies. Cu-Co sulfides are more voluminous in fold hinges at different scales. Brems et al., (2009) showed that in Nkana Central and South, the location of the highest grade ore bodies generally corresponds to the hinge zones of 2nd and 3rd order folds (Fig. 10F). Significant volumes of ore also occur within several generations of veins, syn-kinematic to the folds (Torremans et al., 2014) as well as with volumetrically large veins (>10 cm wide) that are late-kinematic to the folds (Brems et al., 2009; Muchez et al., 2010; Van Wilderode et al., 2015). Low-angle reverse and high-angle normal faults as recognized in our study are not associated with large amounts of sulfides.

6. Interpretation

6.1 Lithofacies variation

The strong lithofacies variations recognized in the COM in the Chambishi-Nkana Basin are consistent with other studies, indicating that sediment deposition in the Mindola Clastics Formation and COM was strongly determined by fault-bounded subbasins with half-graben geometries (Garlick 1961b; Mendelsohn 1961; Fleischer et al., 1976; Selley et al., 2005). The COM represents the first transgression across this compartmentalized depositional environment (Annels 1989; Porada and Druschel 2010; Bull et al., 2011). Later on, more laterally similar conditions developed basinwide, as evidenced by similarities in Rokana Evaporites and overlying units throughout the Nkana region (cf. Bull et al., 2011).

6.2 Development of foliation fabrics

The S_1 cleavage is always parallel to bedding and interpreted as a burial compaction cleavage. Development of the tectonic S_2 cleavage is interpreted as co-genetic with folding, based on the following observations. Throughout the area, S_2 is always axial planar to the local folds. Moreover, in all crosscuts, the π-axis-to-S_1-cleavage lies on the mean S_2 plane to within 5 degrees deviation (Fig. 4). The attitude of Li corresponds quite well to calculated π-axis-to-S_1-cleavage for each of the separate zones in the Nkana South Open Pit (Fig. 8). Therefore, the variability which is observed in the intersection lineation orientation can be explained by similar variability in the cleavage attitude and by the non-cylindrical nature of the folds.

The strongly clustered sub-vertical mean S_2 cleavage of 229/88 (K = 2.51 and C = 3.05) for all measurements combined (n = 75 in Fig. 12) is consistent with the regional SW-NE structural grain of the orogen (Kampunzu and Cailteux 1999; Porada and Berhorst 2000; Selley et al., 2005). In addition, the combined π-axis-to S_1-cleavage at Nkana lies very close to the mean S_2 cleavage plane, at 229/73 (Fig. 12A, B), indicating a slight NE vergence. Moreover, the mean Li attitude of the combined fold train at the Nkana South open pit deviates only slightly from the orientation of the calculated mean fold axis (Fig. 8). Hence, the folding and S_2 cleavage development are interpreted to have occurred during a single NE-SW oriented shortening event.

6.3 Apparent strain gradients and strain partioning along the eastern limb of the Chambishi-Nkana syncline

The deformation intensity varies significantly over the extent of the study area: numerous tight, isoclinal folds at Nkana South gradually become more open towards the NW, north of Nkana Central and ultimately show broad warping of relatively undisturbed and steeply inclined beds at Mindola. A general strain gradient is therefore identified from NW to SE. This gradient can be explained by a combination of two factors (Fig. 13).

First and foremost, the gradient is a geometric effect: A transect is made through a NW-dipping megascale parasitic fold train. The 1st order syncline dips 20° NW and intersects with a low relief highland topography (Figs. 4 and 13). The hinge zone of

this 1st order syncline is intersected at Nkana South, showing high strain, tight to isoclinal, high amplitude 2nd and 3rd order M-type folds. Parasitic, slightly asymmetric, S and Z-folds are found laterally on its limbs. The distance between folds increases towards the NW as the topography intersects the 1st order fold limb of the Chambishi-Nkana syncline progressively further away from its fold axial plane (Figs. 4 and 13). Ultimately, the Mindola deposit is situated far into the limb of this syncline with widely spaced asymmetric sinuisoidal indents in the outcrop pattern of the Upper Roan Group between Nkana Central and Mindola open pit (Figs. 4 and 13).

Secondly, a strong lithofacies variation lies parallel to the strain gradient (cf. Fig. 4), leading to a change in the macroscale build-up of the multilayer sequence. The COM is characterized by strongly cemented, competent, sub- to intertidal dolomites at Mindola, but consists of shale or siltstone with a high fissility along S_1 and S_2 at Nkana Central and South. Based on the observations in this study, the carbonaceous mudrock takes up much more of the strain during folding, compared to the argillaceous dolomite. These observations are therefore an indication of strong strain partitioning in multilayer sequences, caused by lithofacies changes within one unit. Other units in the multilayer sequence do not show such strong lithological variations, except perhaps for large thickness variations in the underlying Mindola Clastics Formation, in relation to palaeogeographic highs (Selley et al., 2005; Croaker 2011; Bull et al., 2011; Hitzman et al., 2012). Given the lack of direct observations near the axial trace of the first order fold in the most northern areas (W of Mindola), a discussion point is whether strain intensity in that area is as intense as in the south. If the COM near the axial plane in the northern part of the study area is similar to the argillaceous dolomite at Mindola (broadly expected based on mapping of the lithofacies in Fig. 4), compressive strain would be more evenly distributed across the whole layer Katanga Supergroup package, and less partitioned into the COM compared to the south (Fig. 13). Small mafic gabbroic to dioritic bodies are regionally widespread and could potentially influence the deformation style locally (Figs. 1, 2 & 4). Unfortunately, we did not encounter mafic bodies in the studied sections, given the sections were in Lower Roan rocks and the mafics occurs predominantly in the Upper Roan and lowermost Nguba Group (Kampunzu et al., 2000).

Analysis of single-layer folded bedding-parallel veins in the carbonaceous mudrock lithofacies of Nkana Central and South showed that the inferred bulk strain from single-layer folding is over 65%, not taking into account prior layer-parallel shortening (Torremans et al., 2014). Microtextural strain analysis of vein fibres revealed additional post-folding homogeneous shortening of 25% in the form of cleavage formation during fold lock-up (Torremans et al., 2014).

Locally, in the carbonaceous mudrock lithofacies of the COM at Nkana Central and South, a significant portioning of the shortening is taken up by cleavage formation. In Mindola, cleavage is not well developed. In the most intensely folded areas (high strain), precipitation of sulphides, quartz, dolomite and mica along disjunctive S_2 cleavage planes indicates that significant pressure solution and diffusion mass transfer must have taken place. The observation that cleavage formation affects syn-folding veins, as well as the geometrical relation between cleavage and folded veins (Figure 7B) indicate that development

of strong spaced disjunctive cleavage in the COM is late-kinematic folding in general, at least after fold-lock up (see detailed analysis in Torremans et al., 2014). These observations, combined with the observation that areas of intense cleavage formation coincide with intensely folded and faulted areas, are evidence of progressive strain partitioning towards certain zones of highly intense deformation.

6.4 Non-cylindricity, interference patterns and strain accommodating mechanisms in folds

Folds at Nkana reveal non-cylindrical elongate periclinal fold geometries, sometimes arranged en-echelon. As there is no evidence for distinct deformation phases, the interference and lateral linking and bifurcation of folds at Nkana is interpreted as linear-linkage, en–echelon-linkage and bifurcation linkage during progressive folding in a single deformation phase (cf. Fig. 10A-C). These types of fold-linkage are mechanically feasible and thought to be a common process during progressive shortening and fold growth (Schmid et al., 2008; Bretis et al., 2011; Grasemann and Schmalholz 2012). Various forms of fold linkage, the existence of culminations and depressions along fold hinges, and curvature of axial planes in multilayer sequences are all shown to be typical phenomena in single-deformation 3D fold development, even in plane strains (Muhlhaus et al., 1998; Schmid et al., 2008; Schmalholz and Schmid 2012; Grasemann and Schmalholz 2012). Plunge variations, structural saddles, and en-echelon periclinal geometries (cf. Fig. 10) all arise from the lateral interactions of growing folds and concomitant angular migration of fold hinges (cf. Treagus and Treagus 1981; Lisle et al., 2010; Hudleston and Treagus 2010). Abundant evidence for bedding-parallel shear is observed. Slickenfibres on bedding-surfaces are reverse slip in normal limbs of the folds (e.g. Fig. 6G, H) and the slip is highest in the limbs of chevron type folds. The slickenline pitch angles are high and coincide with β-girdles of bedding. These observations are all indicative of flexural slip folding (Tanner 1989; Couples et al., 1998). This flexural slip accommodates the 2nd and 3rd order tight to isoclinal chevron type folding producing strongly pinched out hinge zones (e.g. Figures 7C, 8, 9). Conversely, on the 4th order scale in the carbonaceous mudrock of the COM, microstructures in folded bedding-parallel dolomite veins reveal that the main folding mechanism for the veins was flexural flow. Here, the veins behaved as competent beds in an incompetent matrix characterized by a strong rheological contrast (Torremans et al., 2014). Therefore, within one unit at different scales, multiple folding mechanisms may be active simultaneously.

6.5 Timing of faulting

Faults with displacements up to 10 or 20 m were observed in the deposit (Jordaan 1961; Bard and Jordaan 1963; Brems et al., 2009; Croaker 2011). However, based on our observations, fault displacements at the level of the COM are usually much lower. Low and high angle normal and reverse faults are generally observed to be late: They postdate folding and development of S_2, given that faults truncate folded bedding parallel veins (Fig. 7D, E), the relation between faults and S_2 cleavage, and the

lack of folded faults. These faults were therefore activated at least after the fold amplification stage of 4th order folds and during or after late homogeneous shortening of folds (cf. Torremans et al., 2014). We interpret these faults to be related to fold-lockup at high compressional strain. A local NW−SE trending parallelism exists between fault and fold attitudes. Fault attitudes are parallel to bedding strike across 2nd and 3rd order folds, as shown by the coincidence of the π-axis-to-S_1-cleavage and Li with fault planes for several outcrops (e.g. sections 5 and 9 in Figs. 4, 10B). Although no definitive conclusion can be made whether these NW-SE trending faults represent a separate deformation phase or not, this distinct parallelism suggests that folding and later faulting are kinematically linked.

Low-angle reverse faults are consistent with a horizontal NW-SE oriented σ_1 and NW-SE orogenic shortening. Conversely, late high angle normal faults show sub-vertical extensional 'arrowhead' veins along fault planes. Such vein geometries indicate a horizontal NW-SE σ_3 during a phase where the fault was active and are therefore consistent with a late-tectonic inversion towards an extensional Andersonian regime (Cox et al., 2001; Blenkinsop 2008).

7 Discussion

7.1 Synthesis and timing of structural events in the SE Chambishi-Nkana Basin

Basin inversion and compressional deformation are primarily characterized by the development of parasitic fold geometries across 4 orders of scale that form a kinematically coherent system across the length of the southeastern margin of the Chambishi-Nkana Basin. During this phase of parasitic folding, non-cylindrical periclinal fold geometries developed, caused by along-strike interaction of fold geometries as observed by various types of fold linkage structures. These fold geometries, as well as the development of tectonic cleavage can be explained by a single progressive NE-SW oriented shortening event. U–Pb SIMS dating of U-bearing minerals at Nkana that were syntectonic to the shortening revealed ages of 530.1 ± 5.9 Ma (Decrée et al., 2011; Eglinger et al., 2013). In addition, a Re–Os molybdenite age of 525.7 ± 3.4 Ma was obtained for a sample of a chalcopyrite-bearing vein at Nkana that was late-tectonic to the shortening (Barra 2005; Selley et al., 2005). This clearly places the NE-SW oriented shortening event during the Lufilian orogeny. Low angle reverse faults crosscut already folded geometries and represent late stages of orogeny. High angle normal faults are interpreted to represent stress-state inversion towards a vertical effective principal stress after compressional tectonic stresses have waned significantly (Van Noten et al., 2011, 2012).

7.2 Factors influencing fold geometries

The strong lithofacies changes in the COM from competent argillaceous dolomites to incompetent shales or siltstone change the rheology of the multilayer stratigraphy in different parts of the Nkana deposit. These lateral changes in the multilayer

configuration would have significantly influenced the fold characteristics (Muhlhaus et al., 1998; Fischer and Jackson 1999; Frehner and Schmalholz 2006; Tavani et al., 2008; Treagus and Fletcher 2009). Firstly, the higher fissility and intensity of shaly fabric development at Nkana Central and South increases the degree of anisotropy in the multilayer sequence, thereby causing more rapid growth of the fold amplitudes (Price and Cosgrove 1990; Hudleston and Treagus 2010; Hobbs et al., 2011) compared to folds in the argillaceous dolomite lithofacies. Secondly, the amplitudes of parasitic folds steadily decrease from hinge to inflexion points in the larger scale folds (cf. Frehner and Schmalholz 2006). The highest amplitudes are hence seen near the hinge point of the Chambishi-Nkana syncline at Nkana South, diminishing northwards.

The abundant closely spaced competent bedding-parallel veins in the carbonaceous mudrock lithofacies of the COM experienced extremely high amplitude folding (Fig. 6D). High numbers of thin competent layers generate higher amplitude amplification rates than sequences with less layers and therefore develop higher amplitude parasitic folds (Frehner and Schmalholz 2006; Treagus and Fletcher 2009).

The existence of structural saddles and apparent superposition of two fold trend directions has historically been described as "crossfolding" in the Zambian Copperbelt (Garlick 1961b; Bard and Jordaan 1963; Fleischer et al., 1976). More specifically, the NE-SW alignment in culminations and depressions in NW-SE trending fold hinges was often interpreted as the syntax of early NE and late NW directions of folding, attributed to a D3 Chilatembo deformation phase, either late in or posterior to the Lufilian orogeny (Kampunzu and Cailteux 1999; Kampunzu et al., 2009; Kipata et al., 2013). These interpretations must be reassessed, considering newly developed insights into the nature of progressive deformation and fold development (Fletcher 1995; Hudleston and Treagus 2010; Hobbs and Ord 2012; Schmalholz and Schmid 2012) showing that multiple dominant wavelengths and fold hinge line orientations can easily be developed in a progressive folding history (Muhlhaus et al., 1998; Schmid et al., 2008; Hobbs et al., 2011; Grasemann and Schmalholz 2012).

Linking of non-cylindrical periclinal fold geometries is common in deposits with a similar lithostratigraphic architecture throughout the Eastern Zambian Copperbelt, from Konkola in the NW to Luanshya in the SE (See Fig. 2 for locations; Garlick 1961b; Jordaan 1961; Schwellnus 1961; Bard and Jordaan 1963). At the Chambishi mine, fold hinges attain variable NW or SE plunges in overturned 3rd order folds that are arranged en-echelon on the limb of a SW dipping 1st order monoclinal structure (Garlick 1961b). In Chibuluma, fold hinges plunge 7° – 10° towards 330 to 320 (Winfield and Robinson 1963). Various types of fold linkage can be inferred at Chambishi (e.g. Figure 93 in Garlick 1961b). In addition, linkage of 1st order NW and WNW folds occurs at the Luanshya and Baluba deposits (Mendelsohn 1961).

7.3 Strain accommodation during compressional tectonics

Compressional strain accommodation in the Lower Roan during the Lufilian orogeny at Nkana was mainly via folding on multiple scales, with relatively little accommodation of deformation via faulting. The importance of folding is true for most deposits in the Eastern Zambian Copperbelt (Mendelsohn 1961; Selley et al., 2005; Hitzman et al., 2012) except perhaps for Nchanga (Fig. 2), where clear detachment faults and fault-propagation folds are seen, strongly influenced by the presence of the Nchanga granite (McGowan et al., 2003, 2006). In several mines of the Eastern Zambian Copperbelt, areas of intense asymmetric and disharmonic folding have been interpreted to be related to thrusting, with folding above a decoupling zone that has significant layer-parallel shearing (e.g. Luanshya, Nchanga, and Mufulira; McGowan et al., 2003, 2006; Coward & Daly, 1984; Daly et al., 1984). At Nchanga, sheared granite has indeed been thrust into the Lower Roan (Daly et al., 1984). At Nkana, however, we observed no obvious evidence for a decollement or thrusting near the basement-basin interface in the underground exposures, or higher up the sequence. The non-cylindrical parasitic folding is readily explained by rheology contrasts in the multilayer-cake sedimentary sequence during compression. Since it is clear that both basement and Katanga cover were deformed together in the Lufilian orogeny (Coward & Daly, 1984; Daly et al., 1984) and from these different structural styles, it is likely that both basement-involved thrusting as well as rheologically controlled folding processes were active together in the Eastern Zambian Copperbelt. Any large-scale tectonic model therefore needs to carefully assess the contribution of either.

Although there is ample evidence for evaporitic conditions in the Chambishi-Nkana basin, as evident from the lithofacies descriptions (and e.g. Bull et al., 2011), we do not see the effects of salt-driven (detachment) tectonics generating allochtonous pieces of geology. This is in line with other studies in the Eastern Zambian Copperbelt (McCowan et al 2003; Selley et al 2005; Torremans et al., 2013), indicating that salt-tectonics, which are hugely important in many parts the Outer Lufilian in D.R. Congo (e.g. Jackson et al., 2003; Hitzman et al., 2012), are much more subdued or absent in the Eastern Zambian Copperbelt.

When comparing the relative orientation of Li lineations, fold hinge lines, π-poles-to-S_1-cleavage and fault orientation between sections, these structural elements all consistently rotate between sections (Fig. 4). This rotation reflects that of the 1st order syncline from 318° at the SE end of the Basin (e.g. sections 8 and 9; Fig. 4) to c. 300° the northwest of Mindola (Fig. 4). The first possible explanation for this covariation and rotation is that this is a natural consequence of 3D fold growth and linkage, especially since small initial perturbations in palaeo-topography can have a big influence on fold orientation and interaction (Schmid et al., 2008; Bretis et al., 2011; Grasemann and Schmalholz 2012). A second possibility (not excluding elements of the first) is that inherited extensional basin geometries or basement play a significant role in controlling structure development during later shortening (O'Dea and Lister 1995; Holdsworth et al., 1997; Bailey et al., 2002; Potma and Betts 2006).

8 Conclusions

The regional structural analysis on the southeast margin of the Chambishi-Nkana Basin has shown that compressional deformation is characterized by parasitic non-cylindrical NW-SE elongate periclinal fold geometries that strongly interfere laterally, leading to fold linking and bifurcation of folds. In the study area, most of strain was taken up by asymmetric multiscale parasitic folding and not by fault reactivation, fold-thrusting or detachment faulting. Low and high angle reverse faults were observed to be active after the fold amplification stage of 4th order folds and reflect late stages in the orogenic shortening. High angle normal faults are consistent with a late-orogenic stress-state inversion (cf. exhumation and orogenic collapse). The geometrically complex compressional structures are interpreted to have been generated during a single NE-SW oriented shortening event, clearly linked to the Pan-African Lufilian Orogeny. Parasitic fold geometries consistently reflect their position along an inclined NW plunging megascale fold in the SE of the Chambishi-Nkana Basin. Differences in fold amplitude, wavelength and shape are strongly correlated to lateral lithofacies changes in the ore-bearing horizons, interpreted to reflect the influence of mechanical stratigraphy on folding. In addition, the way strain is partitioned within the deforming basin is in large part controlled by the difference in degree of mechanical anisotropy created by the lithofacies variations within the multilayered rock package. These lateral facies changes are an expression of the depositional environment which was characterized by compartmentalized extensional fault-bounded sub-basins and a strong palaeotopography.

Compressional deformation has enriched the ore body on multiple scales, certainly in the carbonaceous mudrock lithofacies of the COM in Nkana South and Central. Grades are higher in fold hinges of 2nd and 3rd order folds, but ore can also be enriched locally, during deformation of competent bedding-parallel veins. In addition, significant volumes of ore occur in several generations of veins that are syn- to late-kinematic to folding, as well as along tectonic S2 cleavage. These observations highlight the potential effects of compressional deformation on ore grades in the fine-grained siliciclastic-hosted Cu-Co orebodies in the Eastern Middle Lufilian. This work provides an essential backdrop to further our understanding of the influence of the Lufilian orogeny on metal mineralization and (re–)mobilization in the Central African Copperbelt.

Competing interests. The authors declare that they have no conflict of interest.

Acknowledgements. The authors thank Osbert Sikazwe, Willy Nundwe and the School of Mines of the University of Zambia for logistic support. We also thank Mopani Mines Plc. for access to the research area and the geologists at Mopani for logistical assistance and many interesting discussions, in particular Wellington Mukumba, Benny Shikwe, Chanda Luwimba, George Chilufya, Stanley Chasauka, Morden Hangoma, Whiteson Silondwa, Lazarus Mwelwa, Emanuel Mwampokota, Mumba Freda and Kennedy Mpolwa. We are grateful to Jorik Van Wilderode and David Debruyne for assistance during field work and stimulating discussions on the geology, metallogenesis and vein forming mechanisms at Nkana. We thank two anynomous reviewers for their helpful and constructive reviews and Bernhard Grasemann for editorial handling. We are grateful to Dave

Wood and Rob Scott for their critical, constructive and helpful reviews of a previous version of this manuscript. This research was financially supported by research grant OT/11/038 of the KU Leuven Bijzonder Onderzoeksfonds.

References

Annels, A. E.: Ore genesis in the Zambian Copperbelt, with particular reference to the Northern Sector of the Chambishi Basin, in: Sediment-hosted stratiform copper deposits, edited by: R. W. Boyle, A. C. Brown, C. W. Jeferson, E. C. Jowett, and R. V. Kirkham, Geological Society of Canada., 427–452, 1989.

Armstrong, R. A., Master, S. and Robb, L. J.: Geochronology of the Nchanga Granite, and constraints on the maximum age of the Katanga Supergroup, Zambian Copperbelt, J. African Earth Sci., 42(1–5), 2005.

Bailey, C. M., Giorgis, S. and Coiner, L.: Tectonic inversion and basement buttressing: an example from the central Appalachian Blue Ridge province, J. Struct. Geol., 24(5), 925–936, doi:10.1016/S0191-8141(01)00102-X, 2002.

Bard, P. G. and Jordaan, J.: Some structural features associated with the Rokhana orebodies, in: Stratiform Copper Deposits in Africa, 2nd Part: Tectonics, Association of African Geological Surveys, Paris, 179–191, 1963.

Barra, F., Broughton, D., Ruiz, J. and Hitzman, M.: Multi-stage mineralization in the Zambian Copperbelt based on Re-Os constraints, Geological Society of America Denver Annual Meeting, Denver, Colorado, USA, Abstracts with Programs, 516, 2004.

Barra, F. L.: Applications of the Re-Os isotopic system in the study of mineral deposits: geochronology and source of metals, Ph.D. thesis, University of Arizona, United States of America, 211 pp., 2005.

Barron, J., Broughton, D., Armstrong, R. A. and Hitzman, M.: Petrology, geochemistry and age of gabbroic bodies in the Solwezi area, northwestern Zambia, in: Proterozoic Sediment-hosted Base Metal Deposits of Western Godwana, Contributions Presented at the 3rd IGCP-450 Conference and Guide Book of the Field Workshop, Lubumbashi, 75–77, 2003.

Batumike, M. J., Kampunzu, A. B. and Cailteux, J. H.: Petrology and geochemistry of the Neoproterozoic Nguba and Kundelungu Groups, Katangan Supergroup, southeast Congo: Implications for provenance, paleaweathering and geotectonic setting, J. African Earth Sci., 44, 97–115, 2006.

Batumike, M. J., Cailteux, J. L. H. and Kampunzu, A. B.: Lithostratigraphy, basin development, base metal deposits, and regional correlations of the Neoproterozoic Nguba and Kundelungu rock successions, central African Copperbelt, Gondwana Res., 11(3), 432–447, doi:10.1016/j.gr.2006.04.012, 2007.

Blenkinsop, T. G.: Relationships between faults, extension fractures and veins, and stress, J. Struct. Geol., 30(5), 622–632, 2008.

Brems, D., Muchez, P., Sikazwe, O. and Mukumba, W.: Metallogenesis of the Nkana copper–cobalt South Orebody, Zambia, J. African Earth Sci., 55(3–4), 185–196, doi:10.1016/j.jafrearsci.2009.04.003, 2009.

Bretis, B., Bartl, N. and Grasemann, B.: Lateral fold growth and linkage in the Zagros fold and thrust belt (Kurdistan, NE Iraq), Basin Res., 23(6), 615–630, doi:10.1111/j.1365-2117.2011.00506.x, 2011.

Brock, B. B.: The structural setting of the Copperbelt, in: The geology of the Northern Rhodesian Copperbelt, edited by F. Mendelsohn, 80–105, MacDonald, 1961.

Broughton, D.W., Hitzman, M.W., and Stephens, A.J.: Exploration history and geology of the Kansanshi Cu-(Au) deposit, Zambia, Society of Economic Geologists, Special Publication 9, p. 141–153, 2002.Buffard, R.: Un rift intracontinental du précambrien supérieur : le Shaba méridional (Zaïre) : évolution sédimentaire et tectonique du Supergroupe de Roan au Groupe du Kundelungu inférieur (Supergroupe du Kundelungu), Ph.D. thesis, Université Du Maine, Le Mans, France, 364 pp., 1988.

Bull, S., Selley, D., Broughton, D., Hitzman, M., Cailteux, J., Large, R. and McGoldrick, P.: Sequence and carbon isotopic stratigraphy of the Neoproterozoic Roan Group strata of the Zambian copperbelt, Precambrian Res., 190(1–4), 70–89, doi:10.1016/j.precamres.2011.07.021, 2011.

Cailteux, J., Binda, P. L., Katekesha, W. M., Kampunzu, A. B., Intiomale, M. M., Kapenda, D., Kaunda, C., Ngongo, K., Tshiauka, T. and Wendorff, M.: Lithostratigraphical correlation of the Neoproterozoic Roan Supergroup from Shaba (Zaire) and Zambia, in the central African copper-cobalt metallogenic province, J. African Earth Sci., 19(4), 265–278, doi:10.1016/0899-5362(94)90014-0, 1994.

Cailteux, J. L. H., Kampunzu, A. B., Lerouge, C., Kaputo, A. K. and Milesi, J. P.: Genesis of sediment-hosted stratiform copper–cobalt deposits, central African Copperbelt, J. African Earth Sci., 42(1–5), 134–158, doi:10.1016/j.jafrearsci.2005.08.001, 2005.

Cailteux, J. L. H., Kampunzu, A. B. and Lerouge, C.: The Neoproterozoic Mwashya-Kansuki sedimentary rock succession in the central African Copperbelt, its Cu-Co mineralisation, and regional correlations, Gondwana Res., 11(3), 414–431, 2007.

Clara, E.: Petrographic, mineralogical and geochemical study of the Mindola Cu-Co ore deposit, Zambia, KU Leuven., MSc. thesis, KU Leuven, Leuven, Belgium, 102 pp., 2009.

Carr, G.R., Dean, J.A., Korsch, M.J., Mizon, K.J.: A comparative study of the lead isotopic compositions of mineralization, basement rocks and gabbros from the Copperbelt and "Domes" regions of northern Zambia, Unpublished report, Commonwealth Scientific and Industrial Research Organization, Division of Mineralogy and Geochemistry, Sydney, Australia, pp 28, 1987.

Clemmey, H.: Sedimentary geology of a late Precambrian copper deposit at Kitwe, Zambia, in: Gisements Stratiforme et Provinces Cuprifères: Annales de la Société géologique de Belgique, edited by: P. Bartholomé, 255–265, 1974.

Clemmey, H.: A proterozoic lacustrine interlude from the Zambian Copperbelt, in: Modern and Acient Lake Sediments, edited by M. E. Tucker and A. Matter, Blackwell scientific publications, 259–278, 1978.

Cosi, M., De Bonis, A., Gosso, G., Hunziker, J., Martinotti, G., Moratto, S., Robert, J. P. and Ruhlman, F.: Late Proterozoic thrust tectonics, high-pressure metamorphism and uranium mineralization in the Domes Area, Lufilian Arc, Northwestern Zambia, Precambrian Res., 58(1–4), 215–240, doi:10.1016/0301-9268(92)90120-d, 1992.

Couples, G. D., Lewis, H. and Tanner, P. W. G.: Strain partitioning during flexural-slip folding, Geol. Soc. London, Spec. Publ., 127(1), 149–165, doi:10.1144/GSL.SP.1998.127.01.12, 1998.

Coward, M. P. and Daly, M. C.: Crustal lineaments and shear zones in Africa: Their relationship to plate movements, Precambrian Res., 24(1), 27–45, 1984.

Cox, S. F., Knackstedt, M. A. and Braun, J.: Principles of Structural Control on Permeability and Fluid Flow in Hydrothermal Systems, in: Structural Controls on Ore Genesis, Reviews in Economic Geology 14, edited by J. P. Richards and R. M. Tosdal, 1–24, 2001.

Croaker, M. R. D.: Nkana-Mindola sediment-hosted Cu-Co deposit, Zambia, Ph.D. thesis, University of Tasmania, Australia, 363 pp., 2011.

Daly, M. and Unrug, R.: The Muva Supergroup of northern Zambia: a craton to mobile belt sedimentary sequence, Verh. van die Geol. Ver. van Suid-Afrika, 85(3), 155–165, 1982.

Daly, M. C., Chakraborty, S. K., Kasolo, P., Musiwa, M., Mumba, P., Naidu, B., Namateba, C., Ngambi, O. and Coward, M. P.: The Lufilian arc and Irumide belt of Zambia: results of a geotraverse across their intersection, J. African Earth Sci., 2(4), 311–318, 1984.

De Cleyn, A.: Petrographic, mineralogical and geochemical study of the Nkana Cu-Co Central Orebody, Zambia, MSc. thesis, KU Leuven, Leuven, Belgium, 117 pp., 2009.

De Swardt, A. and Drysdall, A.: Precambrian geology and structure in central Northern Rhodesia, Geol. Surv. Zambia Mem., 2, 82 pp., 1964.

De Waele, B., Liégeois, J.-P., Nemchin, A. and Tembo, F.: Isotopic and geochemical evidence of proterozoic episodic crustal reworking within the irumide belt of south-central Africa, the southern metacratonic boundary of an Archaean Bangweulu Craton, Precambrian Res., 148(3–4), 225–256, doi:10.1016/j.precamres.2006.05.006, 2006.

Decrée, S., Deloule, É., De Putter, T., Dewaele, S., Mees, F., Yans, J. and Marignac, C.: SIMS U–Pb dating of uranium mineralization in the Katanga Copperbelt: Constraints for the geodynamic context, Ore Geol. Rev., 40(1), 81–89, doi:10.1016/j.oregeorev.2011.05.003, 2011.

Dewaele, S., Muchez, P., Vets, J., Fernandez-Alonzo, M. and Tack, L.: Multiphase origin of the Cu–Co ore deposits in the western part of the Lufilian fold-and-thrust belt, Katanga (Democratic Republic of Congo), J. African Earth Sci., 46(5), 455–469, doi:10.1016/j.jafrearsci.2006.08.002, 2006.

Eglinger, A., André-Mayer, A.-S., Vanderhaeghe, O., Mercadier, J., Cuney, M., Decrée, S., Feybesse, J.-L. and Milesi, J.-P.: Geochemical signatures of uranium oxides in the Lufilian belt: From unconformity-related to syn-metamorphic uranium deposits during the Pan-African orogenic cycle, Ore Geol. Rev., 54, 197–213, doi:10.1016/j.oregeorev.2013.04.003, 2013.

Eglinger, A., Vanderhaeghe, O., André-Mayer, A. S., Goncalves, P., Zeh, A., Durand, C. and Deloule, E.: Tectono-metamorphic evolution of the internal zone of the Pan-African Lufilian orogenic belt (Zambia): Implications for crustal reworking and syn-orogenic uranium mineralizations, Lithos, 240–243, 167–188, doi:10.1016/j.lithos.2015.10.021, 2016.

Fischer, M. P. and Jackson, P. B.: Stratigraphic controls on deformation patterns in fault-related folds: A detachment fold example from the Sierra Madre Oriental, northeast Mexico, J. Struct. Geol., 21(6), 613–633, doi:10.1016/S0191-8141(99)00044-9, 1999.

Fleischer, V. D., Garlick, W. G. and Haldane, R.: Geology of the Zambian Copperbelt: Handbook of strata-bound and stratiform ore deposits, edited by K. H. Wolf, Amsterdam, Elsevier, 506 pp., 1976.

Fletcher, R. C.: Three-dimensional folding and necking of a power-law layer: are folds cylindrical, and, if so, do we understand why?, Tectonophysics, 247(1–4), 65–83, doi:10.1016/0040-1951(95)00021-E, 1995.

Francois, A.: La structure tectonique du katanuien dans la region de Kolwezi (Shaba, Rep. du Zaire), Ann. la Société Géologique Belgique, 116(1), 87–104, 1993.

Frehner, M. and Schmalholz, S. M.: Numerical simulations of parasitic folding in multilayers, J. Struct. Geol., 28(9), 1647–1657, doi:10.1016/j.jsg.2006.05.008, 2006.

Frimmel, H. E., Basei, M. S. and Gaucher, C.: Neoproterozoic geodynamic evolution of SW-Gondwana: a southern African perspective, Int. J. Earth Sci., 100(2–3), 323–354, doi:10.1007/s00531-010-0571-9, 2011.

Garlick, W. G.: Chambishi, in The geology of the Northern Rhodesian Copperbelt, edited by F. Mendelsohn, MacDonald, London., 281–296, 1961a.

Garlick, W. G.: Muva System, in The geology of the Northern Rhodesian Copperbelt, edited by F. Mendelsohn, MacDonald, London., 21–29, 1961b.

Ghosh, S. K. and Ramberg, H.: Buckling experiments on intersecting fold patterns, Tectonophysics, 5(2), 89–105, 1968.

Grasemann, B. and Schmalholz, S. M.: Lateral fold growth and fold linkage, Geology, 40(11), 1039–1042, doi:10.1130/G33613.1, 2012.

Grohmann, C. H. and Campanha, G. A.: OpenStereo: Open Source, Cross-Platform Software for Structural Geology Analysis, in AGU Fall Meeting., 2010.

Haest, M. and Muchez, P.: Stratiform and vein-type deposits in the Pan-African Orogen in Central and Southern Africa: evidence for multiphase mineralisation, Geol. Belgica, 14(1–2), 23–44, 2011.

Hanson, R. E., Wardlaw, M. S., Wilson, T. J. and Mwale, G.: U-Pb zircon ages from the Hook granite massif and Mwembeshi dislocation: constraints on Pan-African deformation, plutonism, and transcurrent shearing in Central Zambia, Precambrian Res., 63(3–4), 189–209, doi:10.1016/0301-9268(93)90033-X, 1993.

Hitzman, M. W., Broughton, D., Selley, D., Woodhead, J., Wood, D. and Bull, S.: The Central African Copperbelt: Diverse Stratigraphic, Structural, and Temporal Settings in the World' s Largest Sedimentary Copper District, Econ. Geol. Spec. Publ. 16, 16, 487–514, 2012.

Hobbs, B. E. and Ord, A.: Localized and chaotic folding: the role of axial plane structures., Philos. Trans. R. Soc. Ser. A Math. Phys. Eng. Sci., 370(1965), 1966–2009, doi:10.1098/rsta.2011.0426, 2012.

Hobbs, B. E., Ord, A. and Regenauer-Lieb, K.: The thermodynamics of deformed metamorphic rocks: A review, J. Struct. Geol., 33(5), 758–818, doi:10.1016/j.jsg.2011.01.013, 2011.

Holdsworth, R. E., Butler, C. A. and Roberts, A. M.: The recognition of reactivation during continental deformation, J. Geol. Soc. London, 154, 73–78, 1997.

Hudleston, P. J. and Treagus, S. H.: Information from folds: A review, J. Struct. Geol., 32(12), 2042–2071, doi:10.1016/j.jsg.2010.08.011, 2010.

Jackson, M. P. A., Warin, O. N., Woad, G. M. and Hudec, M. R.: Neoproterozoic allochthonous salt tectonics during the Lufilian orogeny in the Katangan Copperbelt, Central Africa, Geol. Soc. Am. Bull., 115(3), 314–330, 2003.

John, T., Schenk, V., Mezger, K. and Tembo, F.: Timing and PT evolution of whiteschist metamorphism in the Lufilian Arc-Zambezi Belt orogen (Zambia): Implications for the assembly of Gondwana, J. Geol., 112(1), 71–90, 2004.

Johnson, S. P., Rivers, T. and De Waele, B.: A review of the Mesoproterozoic to early Palaeozoic magmatic and tectonothermal history of south–central Africa: implications for Rodinia and Gondwana, J. Geol. Soc. London, 162(3), 433–450, 2005.

Jordaan, J.: Nkana, in: The geology of the Northern Rhodesian Copperbelt, edited by F. Mendelsohn, MacDonald, London, 297–328, 1961.

Kampunzu, A. B. and Cailteux, J. L. H.: Tectonic evolution of the Lufilian Arc (Central Africa Copper Belt) during Neoproterozoic Pan African orogenesis, Gondwana Res., 2(3), 401–421, 1999.

Kampunzu, A. B., Kapenda, D. and Manteka, B.: Basic magmatism and geotectonic evolution of the Pan African belt in central Africa: Evidence from the Katangan and West Congolian segments, Tectonophysics, 190, 363–371, 1991.

Kampunzu, A. B., Tembo, F., Matheis, G., Kapenda, D. and Huntsman-Mapila, P.: Geochemistry and tectonic setting of mafic igneous units in the Neoproterozoic Katangan Basin, Central Africa: implications for Rodinia break-up, Gondwana Res., 3(2), 125–153, doi:10.1016/s1342-937x(05)70093-9, 2000.

Kampunzu, A. B., Cailteux, J. L. H., Kamona, A. F., Intiomale, M. M. and Melcher, F.: Sediment-hosted Zn–Pb–Cu deposits in the Central African Copperbelt, Ore Geol. Rev., 35(3–4), 263–297, doi:http://dx.doi.org/10.1016/j.oregeorev.2009.02.003, 2009.

Key, R. M., Liyungu, A. K., Njamu, F. M., Somwe, V., Banda, J., Mosley, P. N. and Armstrong, R. a.: The western arm of the Lufilian Arc in NW Zambia and its potential for copper mineralization, J. African Earth Sci., 33(3–4), 503–528, doi:10.1016/S0899-5362(01)00098-7, 2001.

Kipata, L. M., Delvaux, D., Sebagenzi, M. N., Cailteux, J. and Sintubin, M.: Pan-African Lufilian arc and its foreland (Katanga, DRC): from orogenic compression to extensional collapse, transpressional inversion and transition to rifting, Geol. Belgica, 16(1–2), 1–17, 2013.

Lisle, R. J., Toimil, N., Aller, J., Bobillo-Ares, N. and Bastida, F.: The hinge lines of non-cylindrical folds, J. Struct. Geol., 32(2), 166–171, doi:10.1016/j.jsg.2009.10.011, 2010.

Master, S., Rainaud, C., Armstrong, R. A., Phillips, D. and Robb, L. J.: Provenance ages of the Neoproterozoic Katanga Supergroup (Central African Copperbelt), with implications for basin evolution, J. African Earth Sci., 42, 41–60, 2005.

McGowan, R. R., Roberts, S., Foster, R. P., Boyce, A. J. and Coller, D.: Origin of the copper-cobalt deposits of the Zambian Copperbelt: An epigenetic view from Nchanga, Geology, 31(6), 497–500, 2003.

McGowan, R. R., Roberts, S. and Boyce, A. J.: Origin of the Nchanga copper-cobalt deposits of the Zambian Copperbelt, Miner. Depos., 40(6–7), 617–638, doi:10.1007/s00126-005-0032-8, 2006.

Mendelsohn, F.: The Geology of the Northern Rhodesian Copperbelt, MacDonald, London., 523 pp., 1961.

Muchez, P., El Desouky, H., Brems, D., De Cleyn, A., Lammens, L., Cailteux, J., Boyce, A., De Muynck, D., Mukumba, W. and Sikazwe, O.: Evolution of Cu-Co mineralizing fluids at Nkana Mine, Central African Copperbelt, Zambia, J. African Earth Sci., 58(3), 457–474, doi:10.1016/j.jafrearsci.2010.05.003, 2010.

Muchez, P., André-Mayer, A.-S., El Desouky, H. A. and Reisberg, L.: Diagenetic origin of the stratiform Cu–Co deposit at Kamoto in the Central African Copperbelt, Miner. Depos., 50(4), 437–447, doi:10.1007/s00126-015-0582-3, 2015.

Muhlhaus, H.-B., Sakaguchi, H. and Hobbs, B. E.: Evolution of three-dimensional folds for a non-Newtonian plate in a viscous medium, Proc. R. Soc. A Math. Phys. Eng. Sci., 454(1980), 3121–3143, doi:10.1098/rspa.1998.0294, 1998.

O'Dea, M. G. and Lister, G. S.: The role of ductility contrast and basement architecture in the structural evolution of the Crystal Creek block, Mount Isa Inlier, NW Queensland, Australia, J. Struct. Geol., 17(7), 949–960, doi:10.1016/0191-8141(94)00117-I, 1995.

Porada, H. and Berhorst, V.: Towards a new understanding of the Neoproterozoic-Early Palaeozoic Lufilian and northern Zambezi Belts in Zambia and the Democratic Republic of Congo, J. African Earth Sci., 30(3), 727–771, doi:10.1016/S0899-5362(00)00049-X, 2000.

Porada, H. and Druschel, G.: Evidence for participation of microbial mats in the deposition of the siliciclastic “ore formation” in the Copperbelt of Zambia, J. African Earth Sci., 58(3), 427–444, doi:10.1016/j.jafrearsci.2010.04.006, 2010.

Potma, W. A. and Betts, P. G.: Extension-related structures in the Mitakoodi Culmination: Implications for the nature and timing of extension, and effect on later shortening in the eastern Mt Isa Inlier, Aust. J. Earth Sci., 53(1), 55–67, doi:10.1080/08120090500432421, 2006.

Price, N. J. and Cosgrove, J. W.: Analysis of Geological Structures, Cambridge University Press, 502 pp., 1990.

Rainaud, C., Master, S., Armstrong, R. A. and Robb, L. J.: Geochronology and nature of the Palaeoproterozoic basement in the Central African Copperbelt (Zambia and the Democratic Republic of Congo), with regional implications, J. African Earth Sci., 42, 1–31, doi:10.1016/j.jafrearsci.2005.08.006, 2005a.

Rainaud, C., Master, S., Armstrong, R. A., Phillips, D. and Robb, L. J.: Monazite U-Pb dating and 40Ar-39Ar thermochronology of metamorphic events in the Central African Copperbelt during the Pan-African Lufilian Orogeny, J. African Earth Sci., 42, 183–199, 2005b.

Ralston, I. T.: Some structural features associated with the Bancroft orebodies, in Symposium of stratiform Copper deposits in Africa, 127–142, Chapter IX, 2nd part Tectonics, Association of African Geological Surveys., 1963.

Ramsay, J. G.: Folding and Fracturing of Rocks, McGraw-Hill, Inc., 562 pp., 1967.

Schmalholz, S. M. and Schmid, D. W.: Folding in power-law viscous multi-layers., Philos. Trans. R. Soc. Ser. A Math. Phys. Eng. Sci., 370(1965), 1798–826, doi:10.1098/rsta.2011.0421, 2012.

Schmid, D. W., Dabrowski, M. and Krotkiewski, M.: Evolution of large amplitude 3D fold patterns: A FEM study, Phys. Earth Planet. Inter., 171(1–4), 400–408, doi:10.1016/j.pepi.2008.08.007, 2008.

Schwellnus, J. E. G.: Bancroft-Nchanga area, in: The geology of the northern Rhodesian Copperbelt, edited by: F. Mendelsohn, Macdonald, London, 214–233, 1961.

Selley, D., Broughton, D., Scott, R. J., Hitzman, M., Bull, S. W., Large, R. R., McGoldrick, P. J., Croaker, M., Pollington, N. and Barra, F.: A new look at the geology of the Zambian Copperbelt, Econ. Geol., 100, 965–1000, 2005.

Sillitoe, R.H., Perelló, J., Creaser, R.A., Wilton, J., Wilson, A.J. and Dawborn, T.: Age of the Zambian Copperbelt, Miner. Depos., 52, 1245-1268, 2017.

Tanner, G. P. W.: The flexural-slip mechanism, J. Struct. Geol., 11(6), 635–655, doi:10.1016/0191-8141(89)90001-1, 1989.

Tavani, S., Storti, F., Salvini, F. and Toscano, C.: Stratigraphic versus structural control on the deformation pattern associated with the evolution of the Mt. Catria anticline, Italy, J. Struct. Geol., 30(5), 664–681, doi:10.1016/j.jsg.2008.01.011, 2008.

Tembo, F., Kampunzu, A. B. and Porada, H.: Tholeiitic magmatism associated with continental rifting in the Lufilian Fold Belt of Zambia, J. African Earth Sci., 28(2), 403–425, doi:10.1016/s0899-5362(99)00012-3, 1999.

Thieme, J. G. and Johnson, R. L.: Geological map of the Republic of Zambia, Scale 1:1000000, Geol. Surv. Zambia, Lusaka, Zambia, 1981.

Torremans, K., Gauquie, J., Boyce, A. J., Barrie, C. D., Dewaele, S., Sikazwe, O. and Muchez, P.: Remobilisation features and structural control on ore grade distribution at the Konkola stratiform Cu–Co ore deposit, Zambia, J. African Earth Sci., 79(0), 10–23, doi:http://dx.doi.org/10.1016/j.jafrearsci.2012.10.005, 2013.

Torremans, K., Muchez, P. and Sintubin, M.: Mechanisms of flexural flow folding of competent single-layers as evidenced by folded fibrous dolomite veins, J. Struct. Geol., 69, 75–90, doi:10.1016/j.jsg.2014.10.002, 2014.

Treagus, J. E. and Treagus, S. H.: Folds and the strain ellipsoid: a general model, J. Struct. Geol., 3(1), 1–17, doi:10.1016/0191-8141(81)90052-3, 1981.

Treagus, S. H. and Fletcher, R. C.: Controls of folding on different scales in multilayered rocks, J. Struct. Geol., 31(11), 1340–1349, doi:10.1016/j.jsg.2009.07.009, 2009.

Turlin, F., Eglinger, A., Vanderhaeghe, O., André-Mayer, A.-S., Poujol, M., Mercadier, J. and Bartlett, R.: Synmetamorphic Cu remobilization during the Pan-African orogeny: Microstructural, petrological and geochronological data on the kyanite-micaschists hosting the Cu(–U) Lumwana deposit in the Western Zambian Copperbelt of the Lufilian belt, Ore Geol. Rev., 75, 52–75, doi:10.1016/j.oregeorev.2015.11.022, 2016.

Van Noten, K., Muchez, P. and Sintubin, M.,: Stress-state evolution of the brittle upper crust during compressional tectonic inversion as defined by successive quartz vein types (High-Ardenne slate belt, Germany), J. Geol. Soc., 168, 407–422, doi: 10.1144/0016-76492010-112, 2011.

Van Noten, K., Van Baelen, H. and Sintubin, M.: The complexity of 3D stress-state changes during compressional tectonic inversion at the onset of orogeny, Geol. Soc. London Spec. Pub., 367, 51–69, doi: 10.1144/SP367.5, 2012.

Van Wilderode, J., Debruyne, D., Torremans, K., Elburg, M. A., Vanhaecke, F., Muchez, P., Balcaen, L., Elburg, M. A., Vanhaecke, F. and Muchez, P.: Metal sources for the Nkana and Konkola stratiform Cu–Co deposits (Zambian Copperbelt): Insights from Sr and Nd isotope ratios, Ore Geol. Rev., 67, 127–138, doi:10.1016/j.oregeorev.2014.11.011, 2015.

Winfield, O. and Robinson, I. C.: The structures of Chibuluma mine, in: Stratiform Copper Deposits in Africa. Association of African Geological Surveys, edited by: J. Lombard and P. Nicolini, Association of African Geological Surveys: Paris, 192–202, 1963.

Woodcock, N. H. and Naylor, M. A.: Randomness testing in three-dimensional orientation data, J. Struct. Geol., 5(5), 539–548, doi:http://dx.doi.org/10.1016/0191-8141(83)90058-5, 1983.

Zientek, M. L., Bliss, J. D., Broughton, D. W., Christie, M., Denning, P. D., Hayes, T. S., Hitzman, M. W., Horton, J. D., Frost-Killian, S., Douglas, J. J., Master, S., Parks, H. L., Taylor, C. D., Wilson, A. B., Wintzer, N. E. and Woodhead, J.: Sediment-hosted stratabound copper assessment of the Neoproterozoic Roan Group, Central African Copperbelt, Katanga basin,

Democratic Republic of the Congo and Zambia, in: U.S. Geological Survey Scientific Investigations Report 2010-5090-T, 162 pp., 2010.

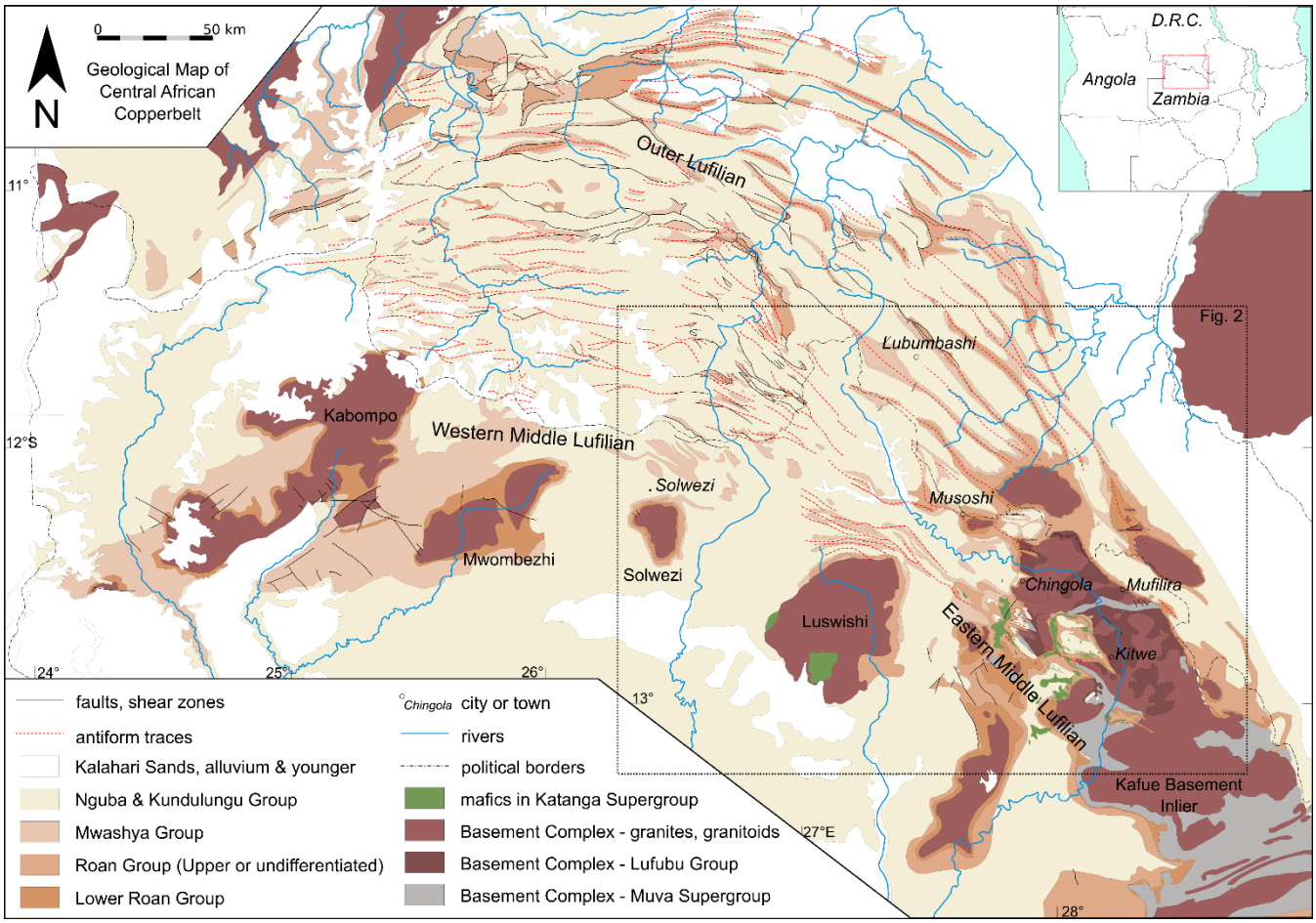

Figure 1: Geological map of the central part of the Central African Copperbelt. Geology is adapted from Thieme and Johnson (1981). Antiform traces are compiled and adapted from Brock (1961), François (1993) and Jackson et al., (Jackson et al., 2003). Basement subdivision in Kafue basement inlier is based on De Waele et al., (2006). Names of the basement inliers are indicated at their respective locations. Inset shows political borders and position in Central Africa.

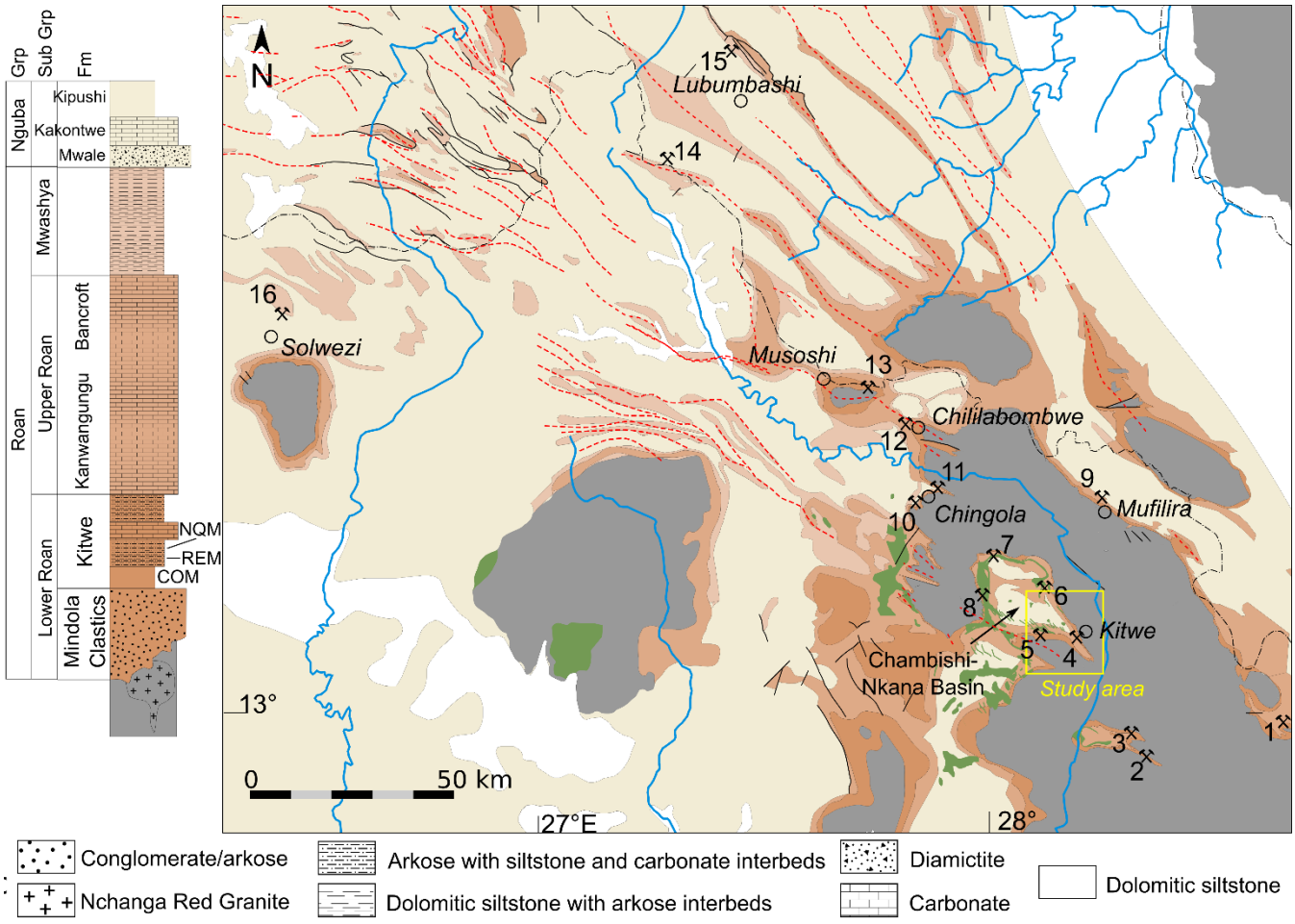

Figure 2: (a) Locations of ore deposits in the Central African Copperbelt that are mentioned in this study. Legend is the same as Fig. 1 except for basement rocks to the Katanga Supergroup that have been combined and are shown in grey. See Fig. 3 for ages of the units. 1: Bwana Mkubwa, 2: Luanshya, 3: Baluba, 4: Nkana South, Central and Mindola, 5: Chibuluma, 6: Chambishi SE, 7: Chambishi, 8: Mwambashi B, 9: Mufilira; 10: Chingola A-F, 11: Nchanga, 12: Konkola, 13: Musoshi, 14: Kipushi, 15: Luiswishi; 16: Kansanshi. (b) Generalized stratigraphic column of the Katanga Supergroup (excluding Kundulungu Grp) and underlying basement rocks (redrawn from Cailteux et al., 1994; Selley et al., 2005; Bull et al., 2011). The predominant lithological characteristics are indicated in symbols. Grp: Group; Sub Grp: Subgroup, Fm: Formation; COM: Copperbelt Orebody Member; NQM: Nchanga Quartzite Member; REM: Rokana Evaporites Member.

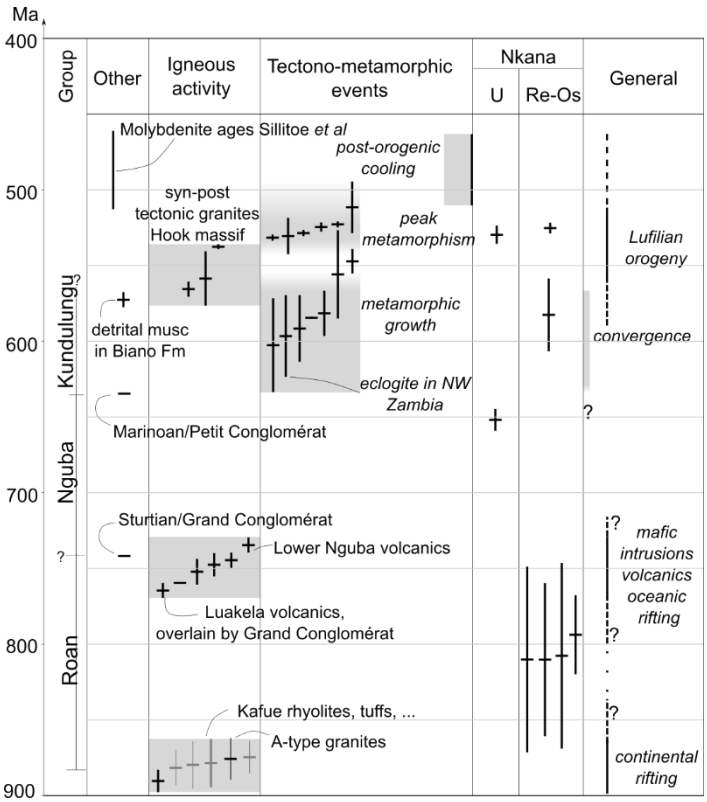

Figure 3: Selected age constraints on tectono-metamorphic events before, during and after deposition of the Katanga Supergroup with interpretation of the major events. Age data are shown with error of 2σ and compiled from Barra et al., (2004), Barra (2005), Muchez et al., (2015) and Eastern Zambian Copperbelt data in Sillitoe et al., (2017) for Re–Os dating; Decrée et al., (2011) for U–Pb dating; Cosi et al., (1992), Hanson et al., (1993), Key et al., (Key et al., 2001), Barron et al., (2003), John et al., (2004), Master et al., (2005); Rainaud et al., (2005b), Armstrong et al., (2005) and Johnson et al., (2005) for various igneous and tectono-metamorphic events and Frimmel et al., (2011) for the timing of the Petit and Grand Conglomérat. The base of the Nguba and Kundulungu Groups are defined by the base of the Grand Conglomérat and the Petit Conglomérat respectively. An overview of the data and references used in this figure is shown in the supplementary material.

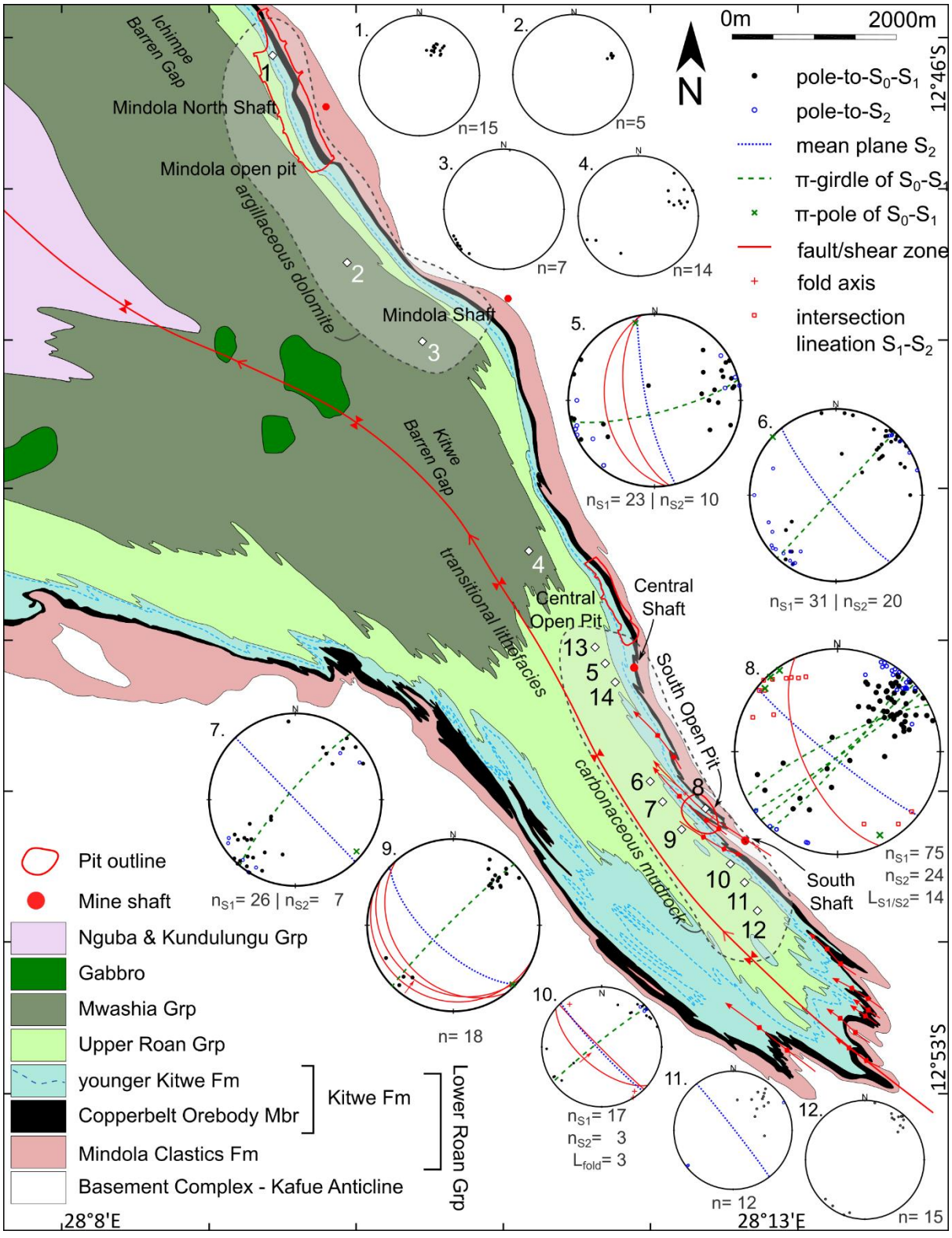
0m
2000m
N
pole-to-S_0-S_1
pole-to-S_2
mean plane S_2
π-girdle of S_0-S_1
π-pole of S_0-S_1
fault/shear zone
fold axis
intersection lineation S_1-S_2
12°46'S
12°53'S
28°8'E
28°13'E
Ichimpe Barren Gap
Mindola North Shaft
Mindola open pit
argillaceous dolomite
Mindola Shaft
Kitwe Barren Gap
transitional lithofacies
Central Open Pit
Central Shaft
South Open Pit
carbonaceous mudrock
South Shaft
1.
n=15
2.
n=5
3.
n=7
4.
n=14
5.
n_{S1}= 23 | n_{S2}= 10
6.
n_{S1}= 31 | n_{S2}= 20
7.
n_{S1}= 26 | n_{S2}= 7
8.
n_{S1}= 75
n_{S2}= 24
$L_{S1/S2}$= 14
9.
n= 18
10.
n_{S1}= 17
n_{S2}= 3
L_{fold}= 3
11.
n= 12
12.
n= 15
Pit outline
Mine shaft
Nguba & Kundulungu Grp
Gabbro
Mwashia Grp
Upper Roan Grp
younger Kitwe Fm
Copperbelt Orebody Mbr
Kitwe Fm
Mindola Clastics Fm
Basement Complex - Kafue Anticline
Lower Roan Grp

Figure 4: Regional structural analysis and lithological variations in the SE of the Chambishi-Nkana Basin. Geological map with indication of the location of mine shafts and open pits mentioned in this study (modified after Mopani Copper Mines Plc. 2009). The numbers indicate the mine sections that were studied in detail. Also indicated on the map is the spatial distribution of the different lithofacies within the COM. Lower-hemisphere equal-area stereoplots show orientation data in the measured sections. Data and statistics on S_1 and S_2 (including β-girdles and π-axes) are given in the supplementary material.

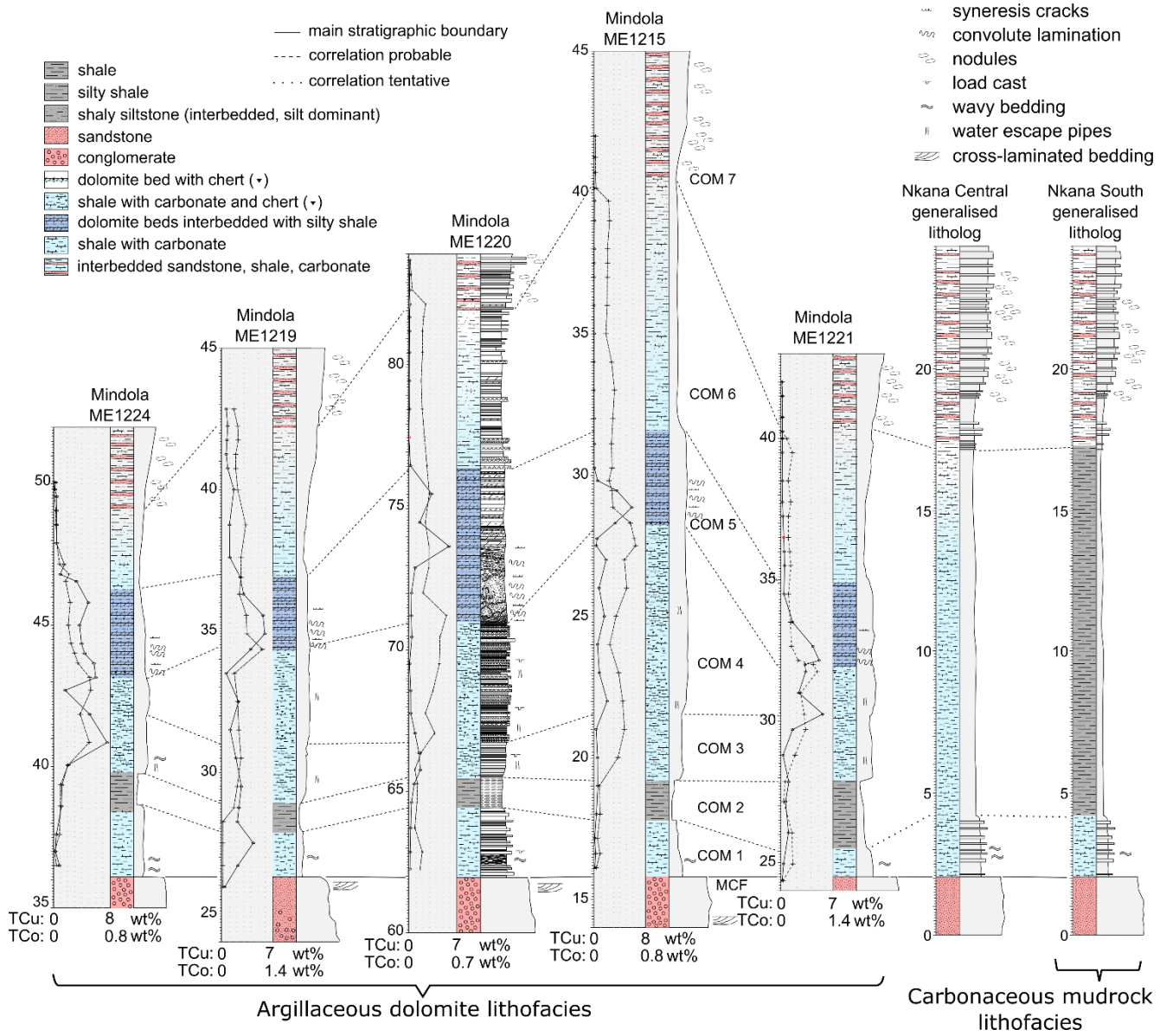

Figure 5: Lithologs of sections at Mindola (typical argillaceous dolomite), Nkana Central and Nkana South (typical carbonaceous mudrock). Log at Mindola is from boreholes ME1220, whereas only composite generalized lithologs are shown for Nkana South and Central, because

of the deformed nature COM there. Correlations are based on observed lithological contacts. Total Cu and Co values in % are given in blue and red respectively, reproduced from data provided by Mopani Copper Mines Plc. These analyses were carried out on drill core halves in sections generally 10 to 15 cm long and averaged over the length of the section. MCF: Mindola Clastics Formation; COM: Copperbelt Orebody Member.

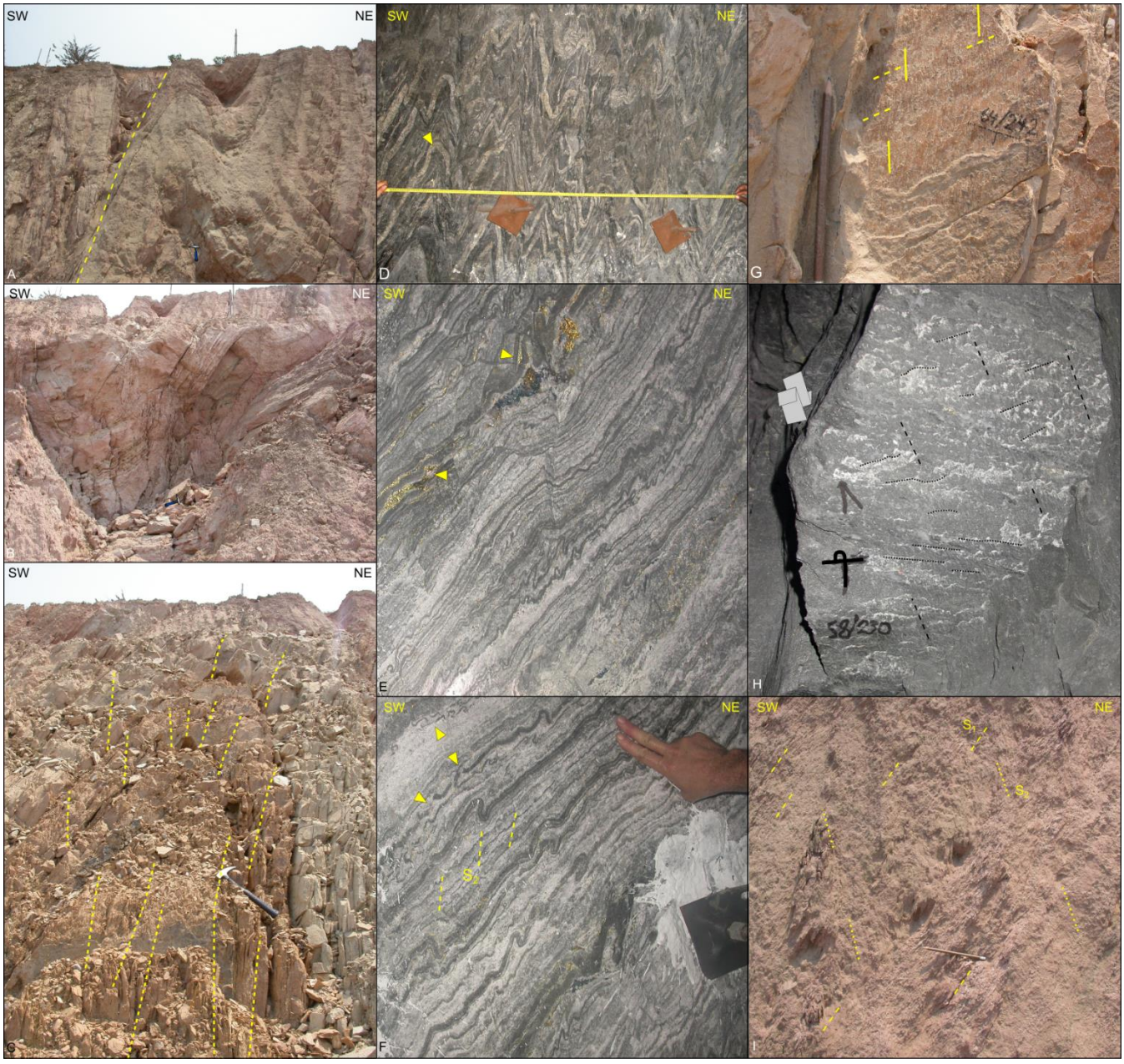

Figure 6: Structural observations at Chambishi-Nkana. See supplementary material for detailed locations. (a–c) Third order folds in the Rokana Evaporites Member. (a) A steep (reverse?) fault developed on the limb of a 3rd order fold. (b) 3rd order parasitic folding in sandstones with a wavelength of around one meter. (c) Slightly NE verging anticline. Almost no cleavage refraction can be observed between beds of the Rokana Evaporites Member. (d–f) Fourth order folding in the COM. (d) High-amplitude folding of bedding-parallel veins in the carbonaceous mudrock lithofacies in section 7. Folds are tight chevron folds, spacing between veins is 2 to 10 cm. (e–f) Intraformational folding of siliciclastic layers (mudstone, siltstone) in dolomite in unit 5 of the argillaceous dolomite at Nkana Mindola. The multilayer folding is poly- to disharmonic. The orientation of the tectonic cleavage is subvertical or dipping steeply NW. Chalcopyrite and bornite occur disseminated and in patches. Occasionally, siliciclastic beds are laterally interrupted or broken up (arrows). (g) Dolomite slickenfibres parallel to S_1 cleavage in the limb of a 3rd order fold developed in the Rokana Evaporites Member in the Nkana South open pit (section 8). Slickenfibre steps reveal reverse slip and the slickenline lineation (pitch of 80; full lines) is sub-orthogonal to the local π-axis-to-S_1-cleavage plunging 9° westwards. Slickenfibre step lineations (dashed lines) are plunging 35 towards 312. (h) Dolomite slickenfibres with steep slickenline lineations (dashed lines) on a S_1 cleavage plane in the limb of a 2rd order fold developed in the COM. The pitch of the dolomite slickenfibre steps (dotted lines) is 26 on the overturned S_1 plane 58/230 in the carbonaceous mudstone in section 6. (i) Carbonaceous mudrock lithofacies of the COM showing a strong bedding-parallel shaly S_1 foliation. A gentle axial planar tectonic cleavage S_2 is developed, by discontinuous alignment of micas and sulfides. The rock is therefore an argillite. Pencil for scale.

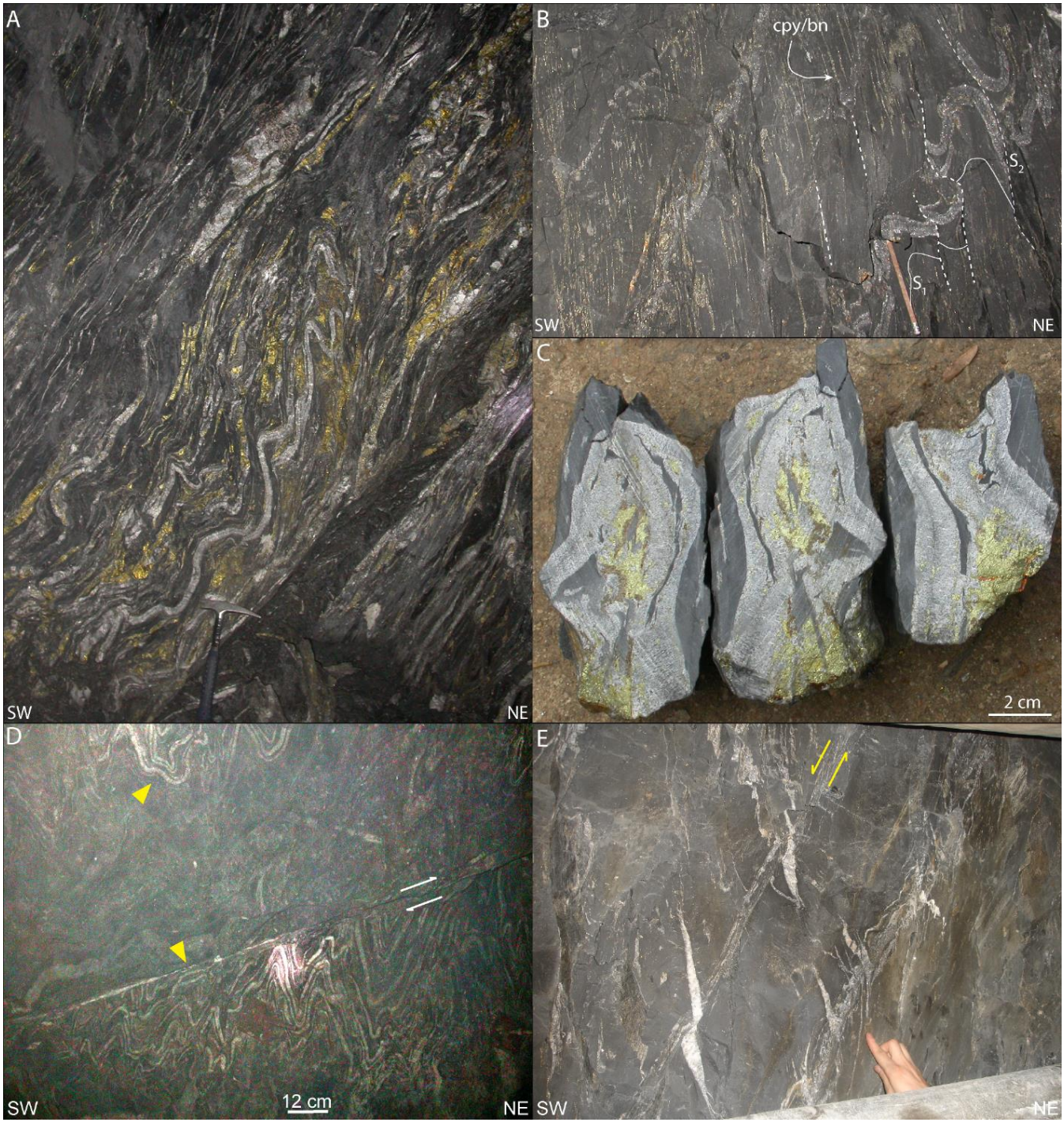
A
SW
NE
B
cpy/bn
S_2
S_1
SW
NE
C
2 cm
D
SW
12 cm
NE
E
SW
NE

Figure 7: See supplementary material for detailed locations. (a) Folded and sheared bedding-parallel veins (type I and II veins of Torremans et al., 2014). Ore mineralization consists of pyrite, chalcopyrite and bornite in the COM and in syn-folding overgrowths. Section 11, 1230S X/C. Note distinct difference in amount of sulfides between the densely veined part and the less-veined parts, suggesting that the folding of the closely spaced competent veins provides accommodation problems and transient permeability for deposition of sulfides. (b) Subvertical disjunctive S_2 cleavage affected folded fibrous bedding-parallel veins. Abundant chalcopyrite, bornite, micas and biotite are found along S_2. Shear slickenfibres are found along some of the S_2 planes. Section 6; 910N X/C. (c) Chalcopyrite, bornite and chalcocite in fold hinges of three parallel cuts through a sample of a 4th order folded fibrous bedding-parallel vein. The axial plane is vertical, at 89/238, with fold limbs oriented 83/238 and 84/058. Section 10; 190S X/C. (d) Low angle reverse fault in 16S crosscut (section 9) displacing folded bedding parallel veins. The fault is orientated 13/203 and mineralized by dolomite and quartz. (e) High angle normal fault with dolomite arrowhead veins in 473N crosscut at section 7 (Fig. 4). Slickenlines indicate an almost purely dip slip shear component. This fault is developed in the southern limb of a 2nd order anticline, with the anticlinal fold hinge towards the right of the photograph.

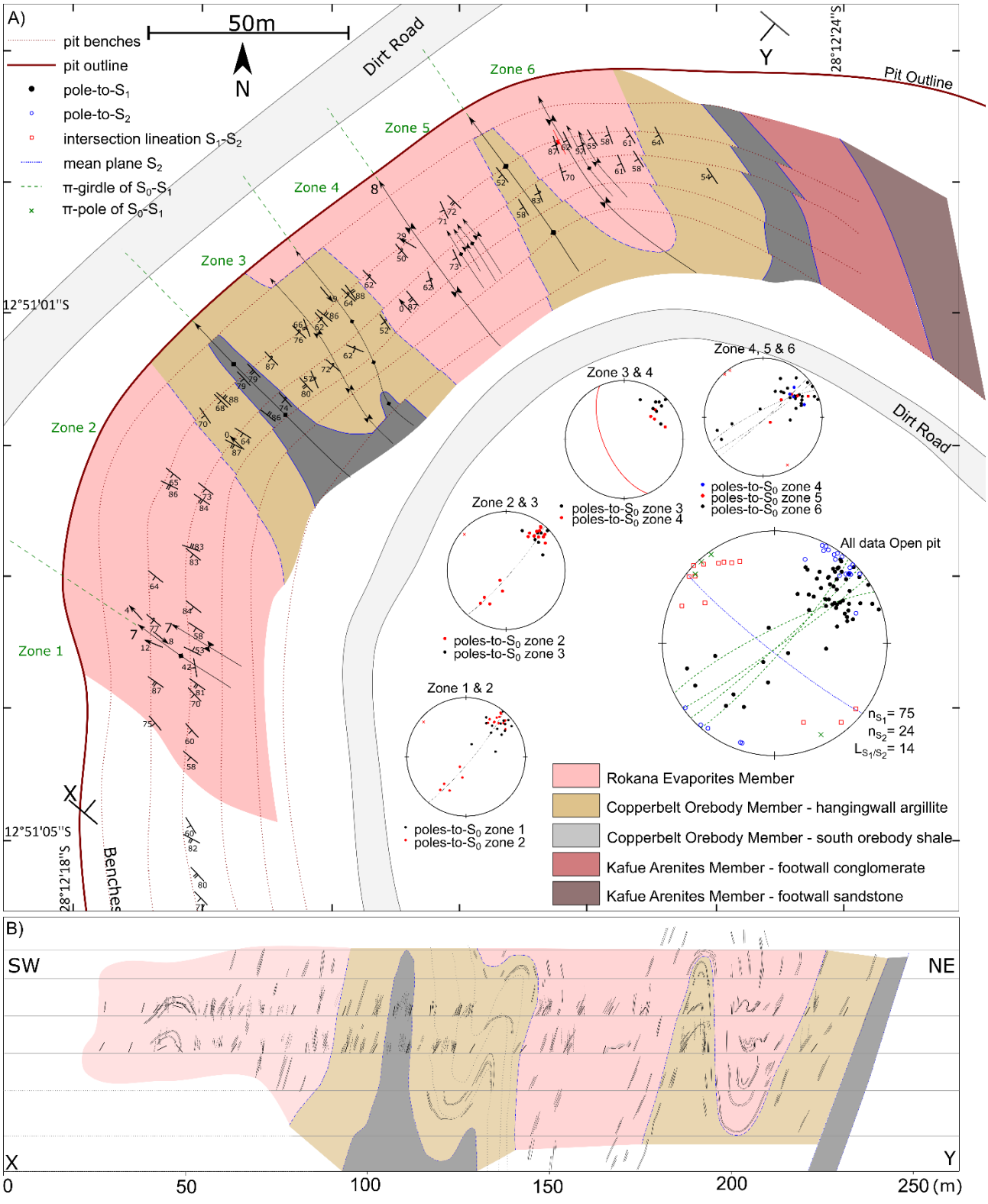
A)
pit benches
pit outline
pole-to-S1
pole-to-S2
intersection lineation S1-S2
mean plane S2
π-girdle of S0-S1
π-pole of S0-S1
50m
N
Dirt Road
Y
28°12'24"S
Pit Outline
Zone 6
Zone 5
Zone 4
Zone 3
Zone 2
Zone 1
12°51'01"S
12°51'05"S
28°12'18"S
X
Benches
Zone 3 & 4
Zone 4, 5 & 6
Zone 2 & 3
Zone 1 & 2
All data Open pit
poles-to-S0 zone 3
poles-to-S0 zone 4
poles-to-S0 zone 4
poles-to-S0 zone 5
poles-to-S0 zone 6
poles-to-S0 zone 2
poles-to-S0 zone 3
poles-to-S0 zone 1
poles-to-S0 zone 2
nS1= 75
nS2= 24
LS1/S2= 14
Rokana Evaporites Member
Copperbelt Orebody Member - hangingwall argillite
Copperbelt Orebody Member - south orebody shale
Kafue Arenites Member - footwall conglomerate
Kafue Arenites Member - footwall sandstone
B)
SW
NE
X
Y
0
50
100
150
200
250 (m)

Figure 8: (a) Geological map of the west side of the Nkana South open pit (section 8). Lower hemisphere equal-area stereoplots refer to particular zones in the pit. Data and statistics on zones, girdles and π-axes-to-S_1-cleavage are given in the supplementary material. (b) Cross-section is perpendicular to the structural trend in the open pit and without height exaggeration.

Figure 9: Cross-section view towards the northwest side of the Nkana South open pit, taken August 14th 2012. See supplementary material for location where photo was taken. The COM is the black layer, showing isoclinal folding and pinched out fold hinges. Compare with Fig. 8B for geology in cross-section.

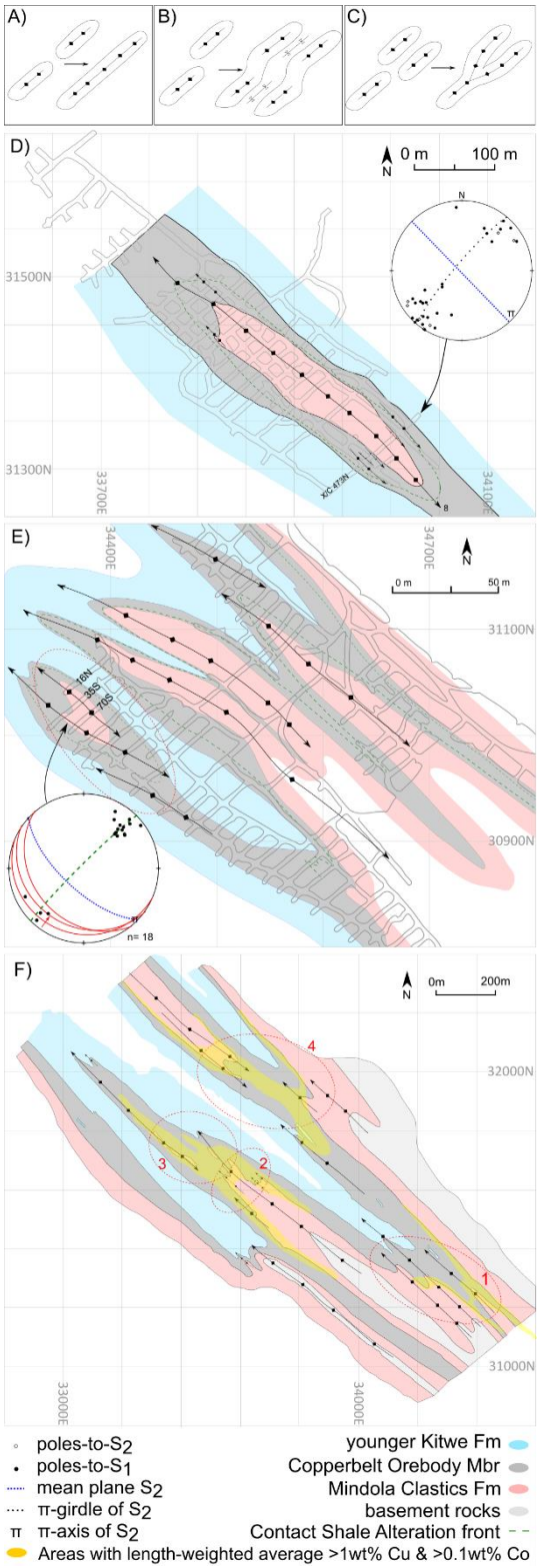
A)
B)
C)
D)
0 m
100 m
N
31500N
31300N
33700E
34100E
XC-473N
E)
34400E
34700E
0 m
50 m
31100N
30900N
16N
38S
78S
n= 18
F)
0m
200m
32000N
31000N
33000E
34000E
1
2
3
4
poles-to-S2
poles-to-S1
mean plane S2
π-girdle of S2
π-axis of S2
Areas with length-weighted average >1wt% Cu & >0.1wt% Co
younger Kitwe Fm
Copperbelt Orebody Mbr
Mindola Clastics Fm
basement rocks
Contact Shale Alteration front

Figure 10: (a–c) Simplified illustration of concepts of fold linkage. (a) Direct fold linkage. (b) En-echelon fold linkage. (c) Bifurcation fold linkage. (d–f) Geological plans of underground levels (*c.* subhorizontal) and equal-area lower hemisphere stereoplots. (d) Geological map of section 7 at 3220L around 473N crosscut in Nkana South. This section intersects a doubly-plunging (periclinal) NW-SE trending 2nd order fold geometry. Several 3rd order parasitic folds are present along the crosscuts. Stereoplot shows measurements in 473N crosscut, with the pole-to-S_1-cleavage plunging 8° towards the SE and axial planar S_2 cleavage. (e) Geological map of section 9 on 3140L at Nkana South. The stereoplot shows several shallow dipping reverse faults trending NW-SE (e.g. Fig. 7D). Folds are tight to isoclinally folded and the COM is often pinched out (cf. like in Fig. 9). The folds are arranged in a right stepping en-echelon system and are slightly periclinal. (f) Published geological plan by Brems *et al.*, (2009) of 3360L in Nkana South, at around the same position of section 8, slightly NE-wards. Areas in yellow are orebodies as defined by Brems *et al.*, (2009), containing >1wt% Cu and 0.1 wt% Co based on length-weighted composite assays from 186 horizontal drillholes. Interpretations of fold axial traces and patterns of geological layer boundaries show several interesting features, indicated by number 1 to 4. At [1], left stepping en-echelon folds are developed. At [2] multiple parasitic folds are developed in the Mindola Clastics Fm, as well as [3] strongly non-cylindrical fold geometries. At [4], a non-cylindrical left stepping en-echelon structure is developed, creating a saddle.

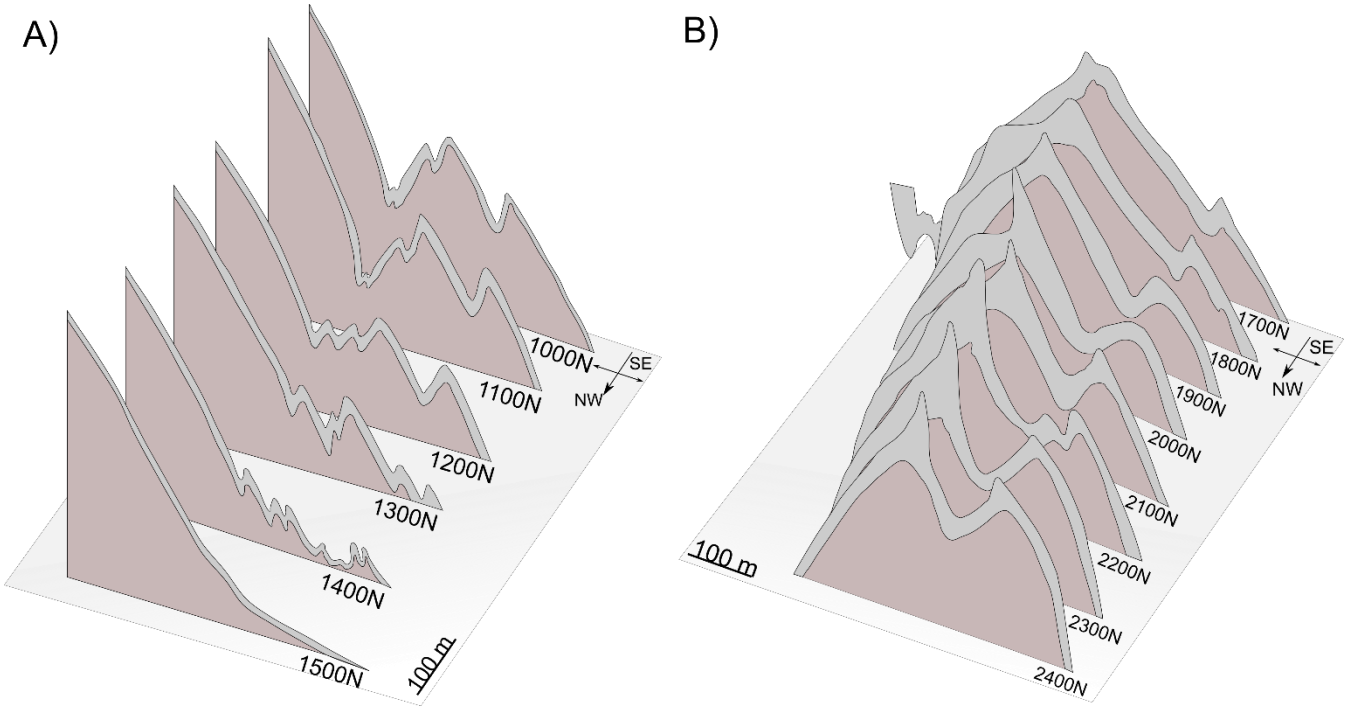

Figure 11: Fence diagrams of cross-sections. View towards the SW of the COM (a) section 13 between 2700L and 3300L (in feet) and between 1700mN and 2400mN in Nkana Central and (b) section 14 between 2500L and 3300L (in feet) and between 1000mN and 1500mN in Nkana Central. The diagrams are based on a reconstruction from geological maps, boreholes and subsection plans of Mopani Mines Plc. in the Vulcan software. The COM is shown in grey and various underlying formations are given in red. The plane in light grey represents the horizontal plan of 3300L level. (a) The COM is strongly pinched out, small parasitic folds evolve into major folds from SE to NW as an en-echelon fold system. (b) In the NE a strongly developed parasitic 2nd order fold is seen with multiple 3rd order folds. This 2nd order fold gradually dies out towards the NW over a distance of *c.* 500 m.

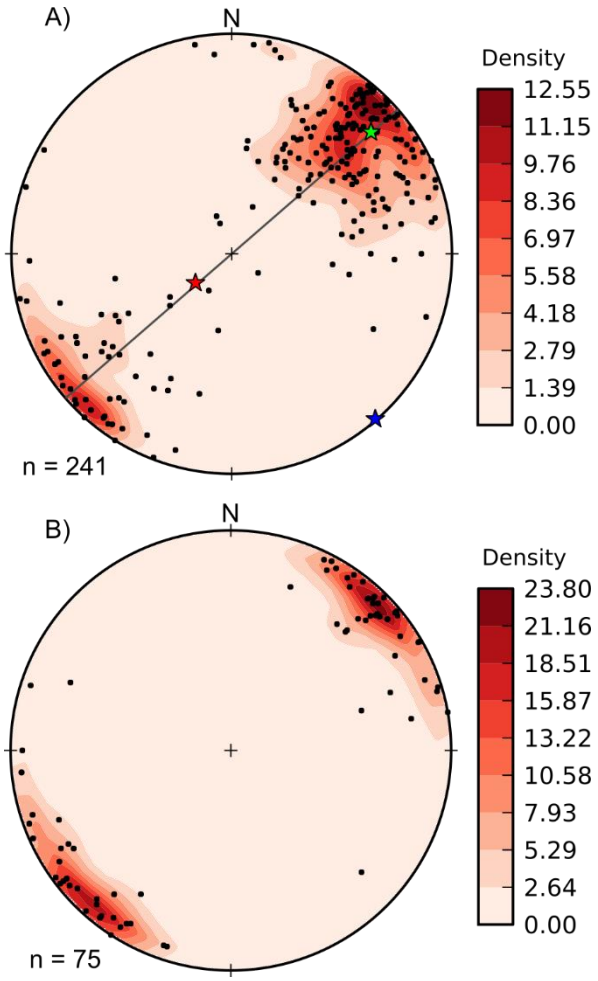

Figure 12: All orientation data at Nkana South, Central and Mindola. Contouring is done by the Fisher distribution. (a) Poles-to-S_1 foliation have a maximum density at 047/07. (b) Poles-to-S_2 foliation have a maximum eigenvector of the distribution at 043/07.

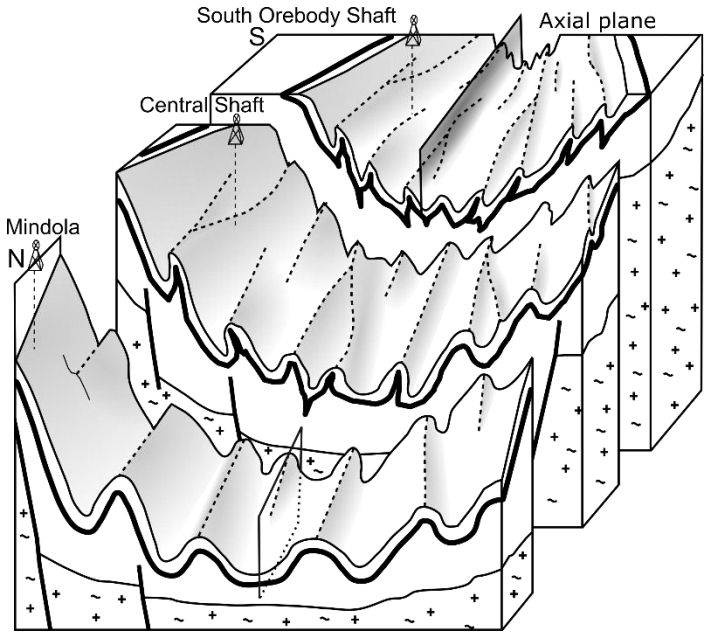

Figure 13: Interpretative schematic block diagram of the SE part of the Chambishi-Nkana Basin, showing 1st order synclinal structure plunging 20 – 30° to the NW. Only Lower Roan Group stratigraphy is shown with the top of the Lower Roan Group exposed and the COM represented by the thick black line. Third order folds are tight to isoclinally folded in the South generally opening up towards the North. The COM at South Orebody behaves ductely and is pinched out or fault-bounded in the fold hinges and folds sometimes plunge southwards. Towards the North, the lithofacies of the COM changes to a more competent unit with the Mindola and Mindola North shafts excavating the north-eastern limb of the second order syncline.

Grp
Sub Grp
Fm
Nguba
Kipushi
Kakontwe
Mwale
Roan
Mwashya
Upper Roan
Bancroft
Kanwangungu
Lower Roan
Kitwe
NQM
REM
COM
Mindola Clastics
N
15
Lubumbashi
14
16
Solwezi
Musoshi
13
Chililabombwe
12
11
9
Mufilira
Chingola
10
7
8
6
5
4
Kitwe
Chambishi-
Nkana Basin
Study area
3
2
1
13°
0
50 km
27°E
28°
Conglomerate/arkose
Nchanga Red Granite
Arkose with siltstone and carbonate interbeds
Dolomitic siltstone with arkose interbeds
Diamictite
Carbonate
Dolomitic siltstone

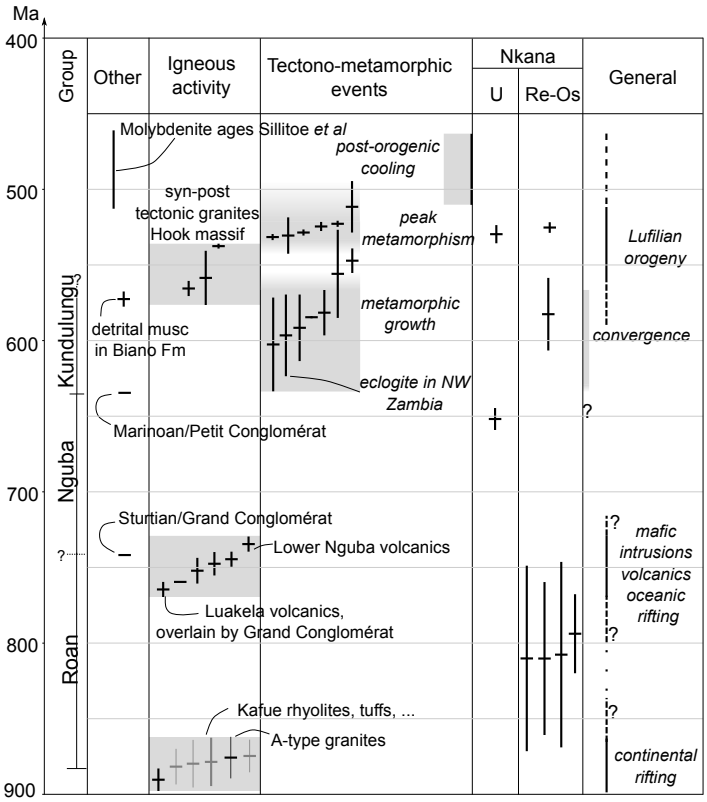
Ma
400
500
600
700
800
900
Group
Other
Igneous activity
Tectono-metamorphic events
Nkana
U
Re-Os
General
Kundulungu
Nguba
Roan
Molybdenite ages Sillitoe et al
post-orogenic cooling
syn-post tectonic granites Hook massif
peak metamorphism
Lufilian orogeny
metamorphic growth
detrital musc in Biano Fm
convergence
eclogite in NW Zambia
Marinoan/Petit Conglomérat
Sturtian/Grand Conglomérat
Lower Nguba volcanics
mafic intrusions
volcanics
oceanic rifting
Luakela volcanics, overlain by Grand Conglomérat
Kafue rhyolites, tuffs, ...
A-type granites
continental rifting

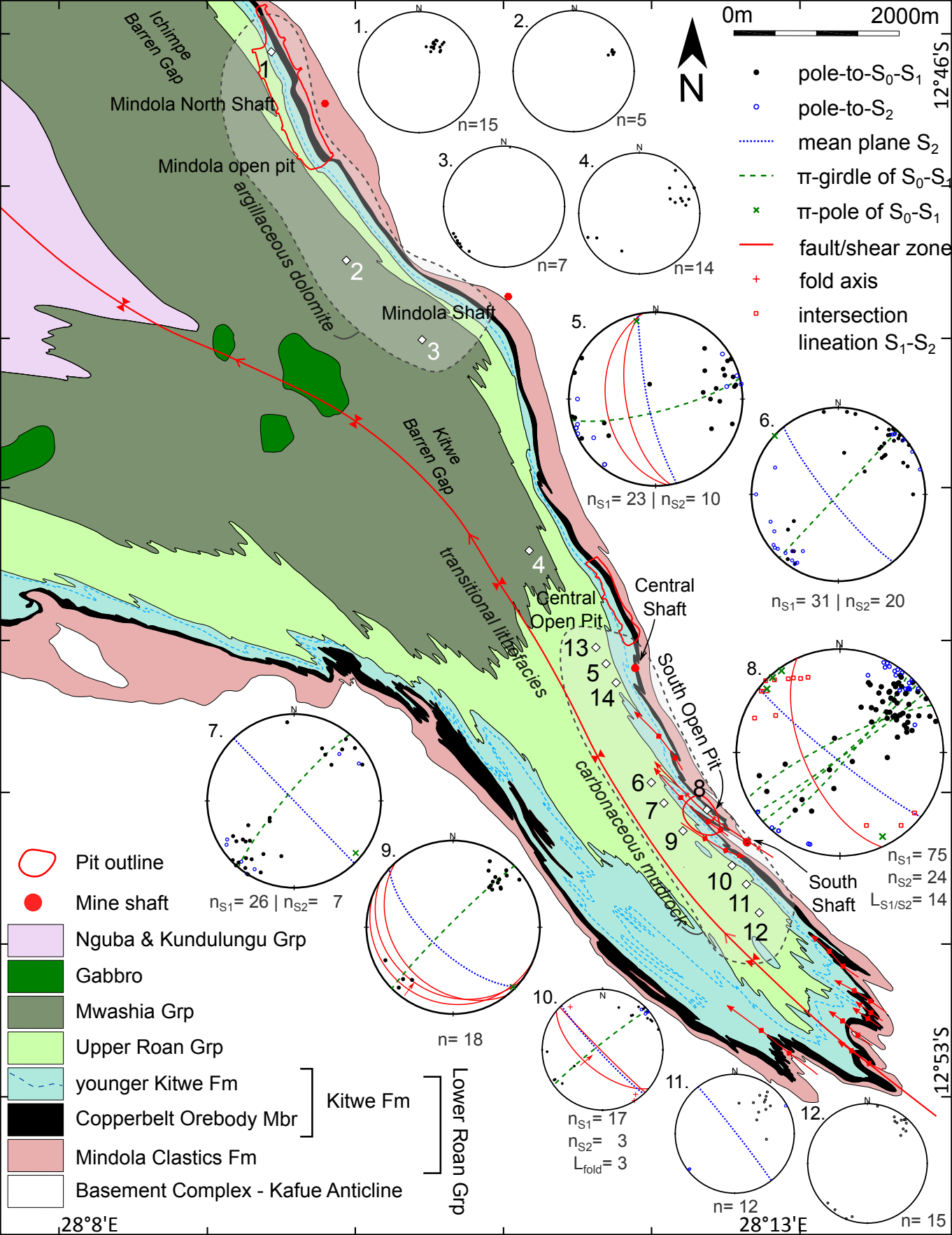
0m
2000m
N
12°46'S
12°53'S
28°8'E
28°13'E
pole-to-S0-S1
pole-to-S2
mean plane S2
π-girdle of S0-S1
π-pole of S0-S1
fault/shear zone
fold axis
intersection lineation S1-S2
Ichimpe Barren Gap
Mindola North Shaft
Mindola open pit
argillaceous dolomite
Mindola Shaft
Kitwe Barren Gap
transitional lithofacies
Central Open Pit
Central Shaft
South Open Pit
carbonaceous mudrock
South Shaft
1.
n=15
2.
n=5
3.
n=7
4.
n=14
5.
nS1= 23 | nS2= 10
6.
nS1= 31 | nS2= 20
7.
nS1= 26 | nS2= 7
8.
nS1= 75
nS2= 24
LS1/S2= 14
9.
n= 18
10.
nS1= 17
nS2= 3
Lfold= 3
11.
n= 12
12.
n= 15
Pit outline
Mine shaft
Nguba & Kundulungu Grp
Gabbro
Mwashia Grp
Upper Roan Grp
younger Kitwe Fm
Copperbelt Orebody Mbr
Kitwe Fm
Mindola Clastics Fm
Basement Complex - Kafue Anticline
Lower Roan Grp

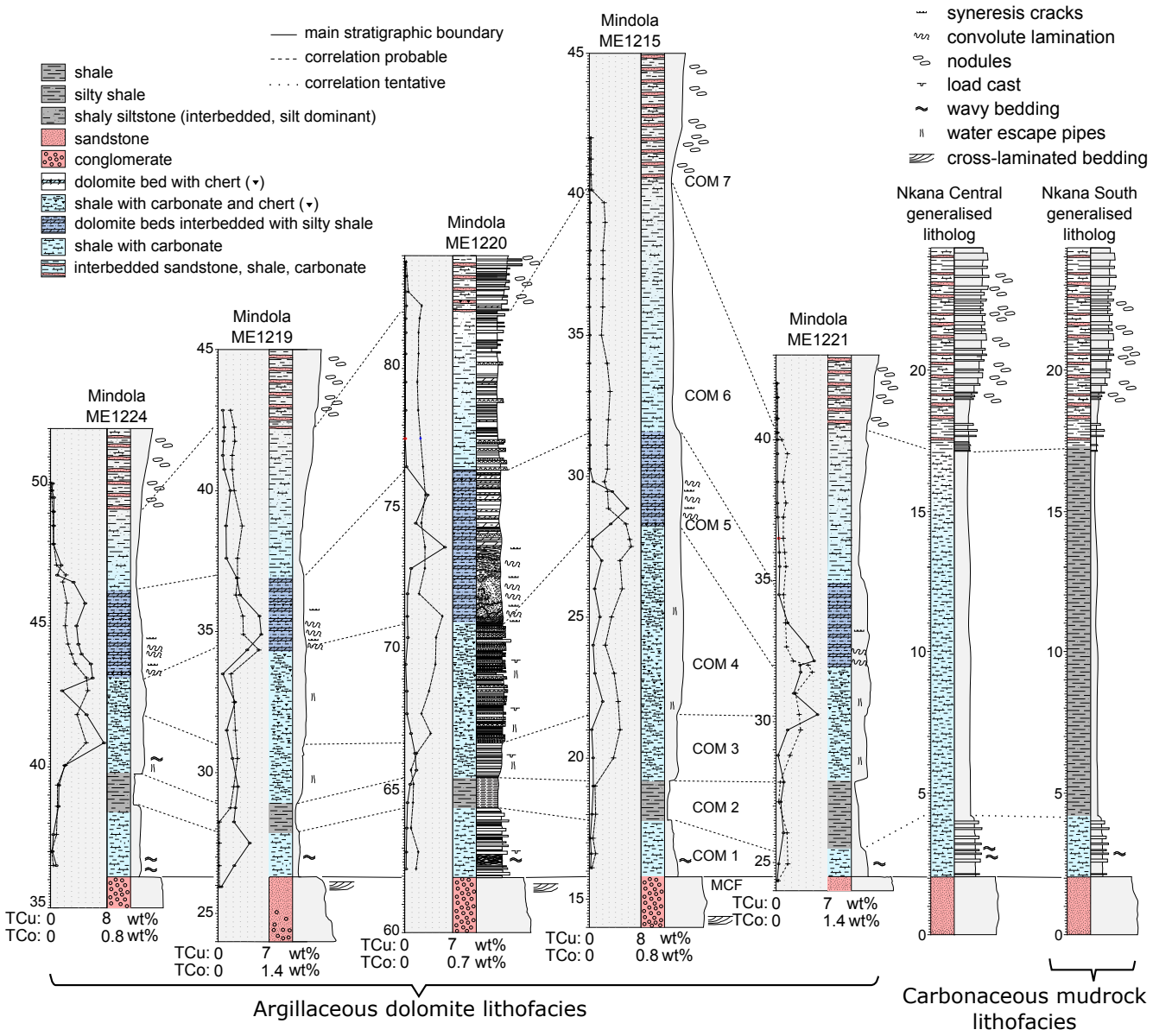
main stratigraphic boundary
correlation probable
correlation tentative
shale
silty shale
shaly siltstone (interbedded, silt dominant)
sandstone
conglomerate
dolomite bed with chert
shale with carbonate and chert
dolomite beds interbedded with silty shale
shale with carbonate
interbedded sandstone, shale, carbonate
syneresis cracks
convolute lamination
nodules
load cast
wavy bedding
water escape pipes
cross-laminated bedding
Mindola ME1224
Mindola ME1219
Mindola ME1220
Mindola ME1215
Mindola ME1221
Nkana Central generalised litholog
Nkana South generalised litholog
COM 7
COM 6
COM 5
COM 4
COM 3
COM 2
COM 1
MCF
TCu: 0
TCo: 0
8 wt%
0.8 wt%
7 wt%
1.4 wt%
7 wt%
0.7 wt%
Argillaceous dolomite lithofacies
Carbonaceous mudrock lithofacies

A)

50m

N

pit benches

pit outline

pole-to-S_1

pole-to-S_2

intersection lineation S_1-S_2

mean plane S_2

π-girdle of S_0-S_1

π-pole of S_0-S_1

Dirt Road

Pit Outline

Zone 1

Zone 2

Zone 3

Zone 4

Zone 5

Zone 6

12°51'01''S

12°51'05''S

28°12'18''S

28°12'24''S

Benches

X

Y

Zone 3 & 4

Zone 4, 5 & 6

Zone 2 & 3

Zone 1 & 2

poles-to-S_0 zone 3
poles-to-S_0 zone 4

poles-to-S_0 zone 4
poles-to-S_0 zone 5
poles-to-S_0 zone 6

poles-to-S_0 zone 2
poles-to-S_0 zone 3

poles-to-S_0 zone 1
poles-to-S_0 zone 2

All data Open pit

n_{S_1}= 75
n_{S_2}= 24
L_{S_1/S_2}= 14

Rokana Evaporites Member

Copperbelt Orebody Member - hangingwall argillite

Copperbelt Orebody Member - south orebody shale

Kafue Arenites Member - footwall conglomerate

Kafue Arenites Member - footwall sandstone

B)

SW

NE

X

Y

0

50

100

150

200

250 (m)

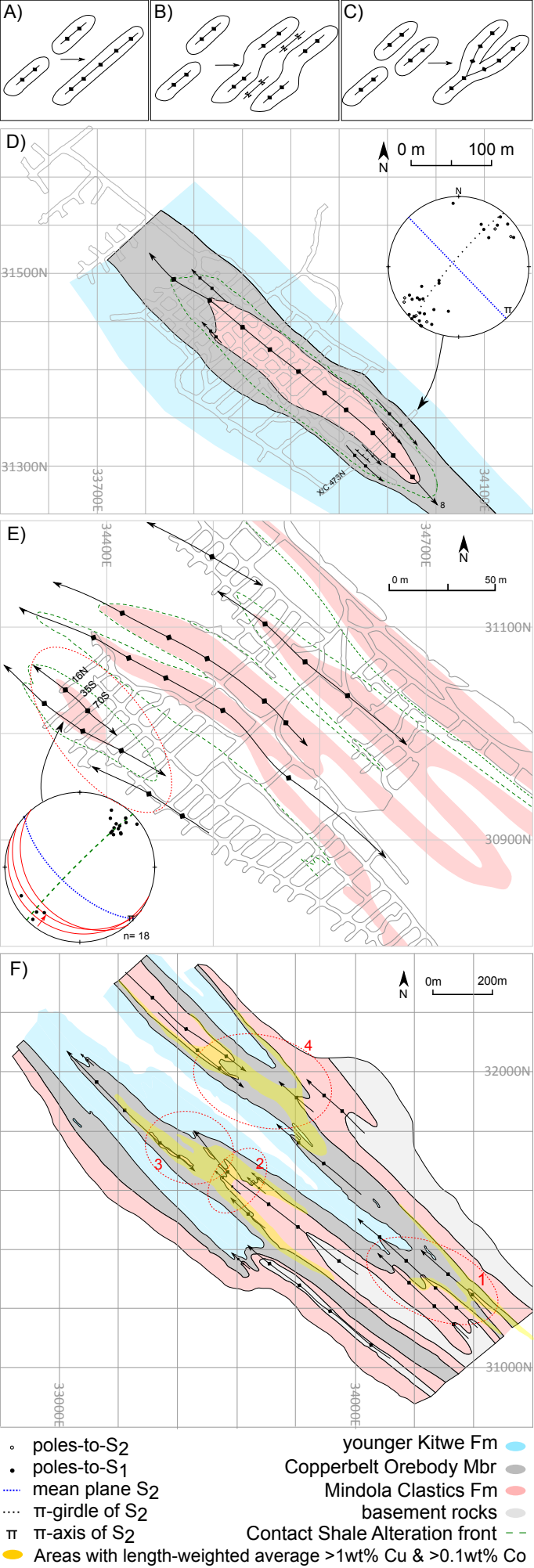

- poles-to-S_2
- poles-to-S_1
- mean plane S_2
- π-girdle of S_2
- π-axis of S_2
- younger Kitwe Fm
- Copperbelt Orebody Mbr
- Mindola Clastics Fm
- basement rocks
- Contact Shale Alteration front
- Areas with length-weighted average >1wt% Cu & >0.1wt% Co

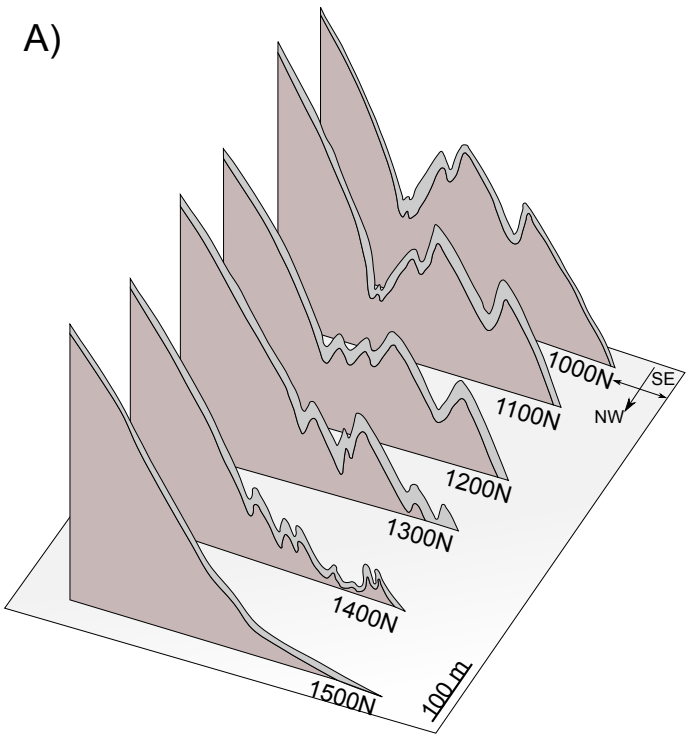
A)
1000N
SE
NW
1100N
1200N
1300N
1400N
1500N
100 m

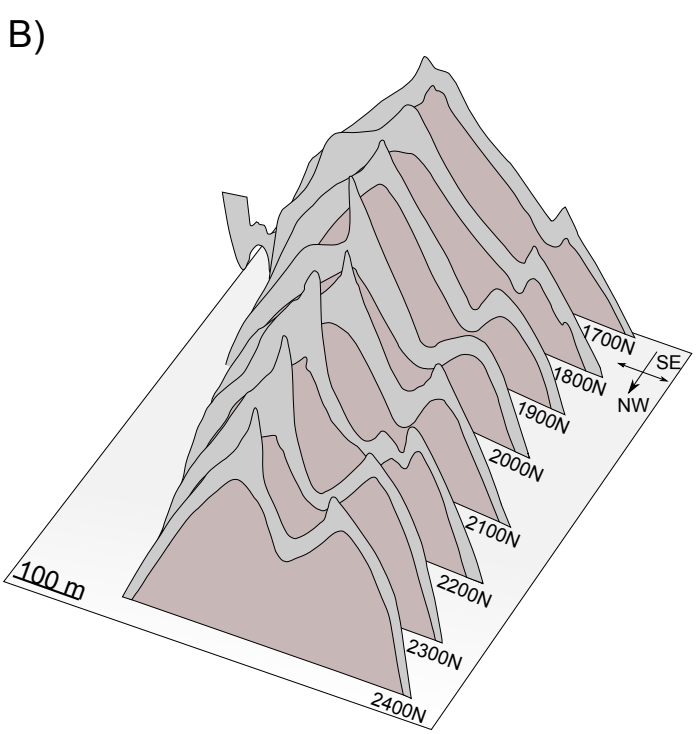
B)
1700N
SE
NW
1800N
1900N
2000N
2100N
2200N
2300N
2400N
100 m

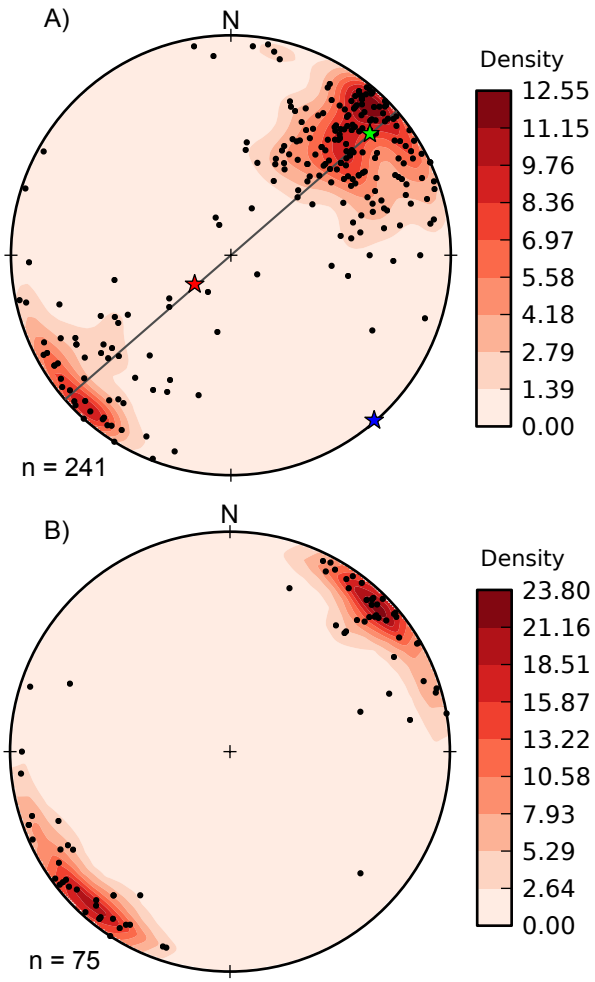
A)
N
Density
12.55
11.15
9.76
8.36
6.97
5.58
4.18
2.79
1.39
0.00
n = 241

B)
N
Density
23.80
21.16
18.51
15.87
13.22
10.58
7.93
5.29
2.64
0.00
n = 75

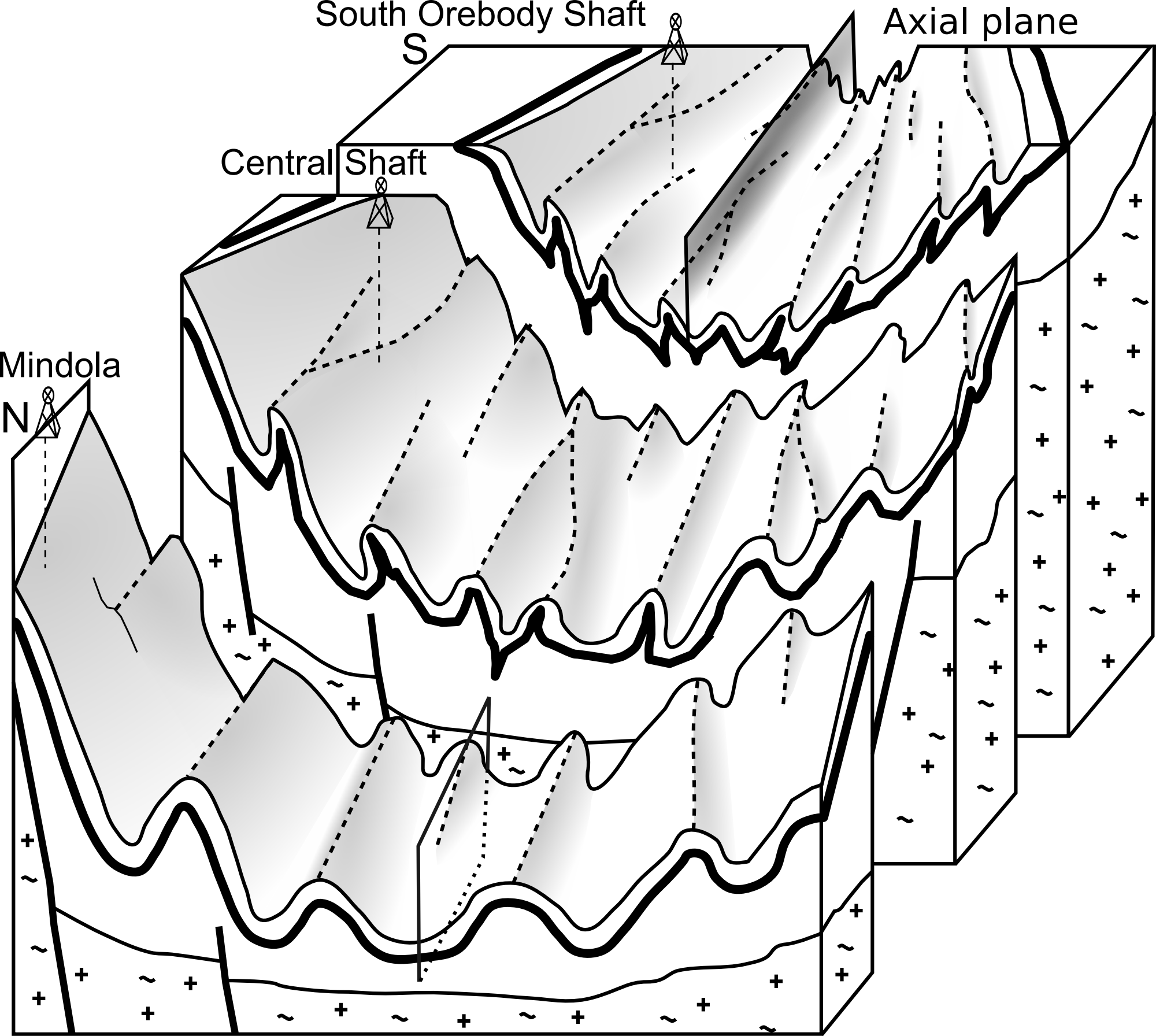
South Orebody Shaft
S
Axial plane
Central Shaft
Mindola
N